AD-A051 092 COMPUTER CODE CONSULTANTS SOLANA BEACH CA F/G 19/4
THREE-DIMENSIONAL COMPUTATIONS, VOLUME IV: 77.5 DEGREES OBLIQUE--ETC(U)
DEC 77 W JOHNSON, V KUCHER DAAD05-76-C-0755

UNCLASSIFIED ARBRL-CR-356 NL

| OF |
AD
A051 092

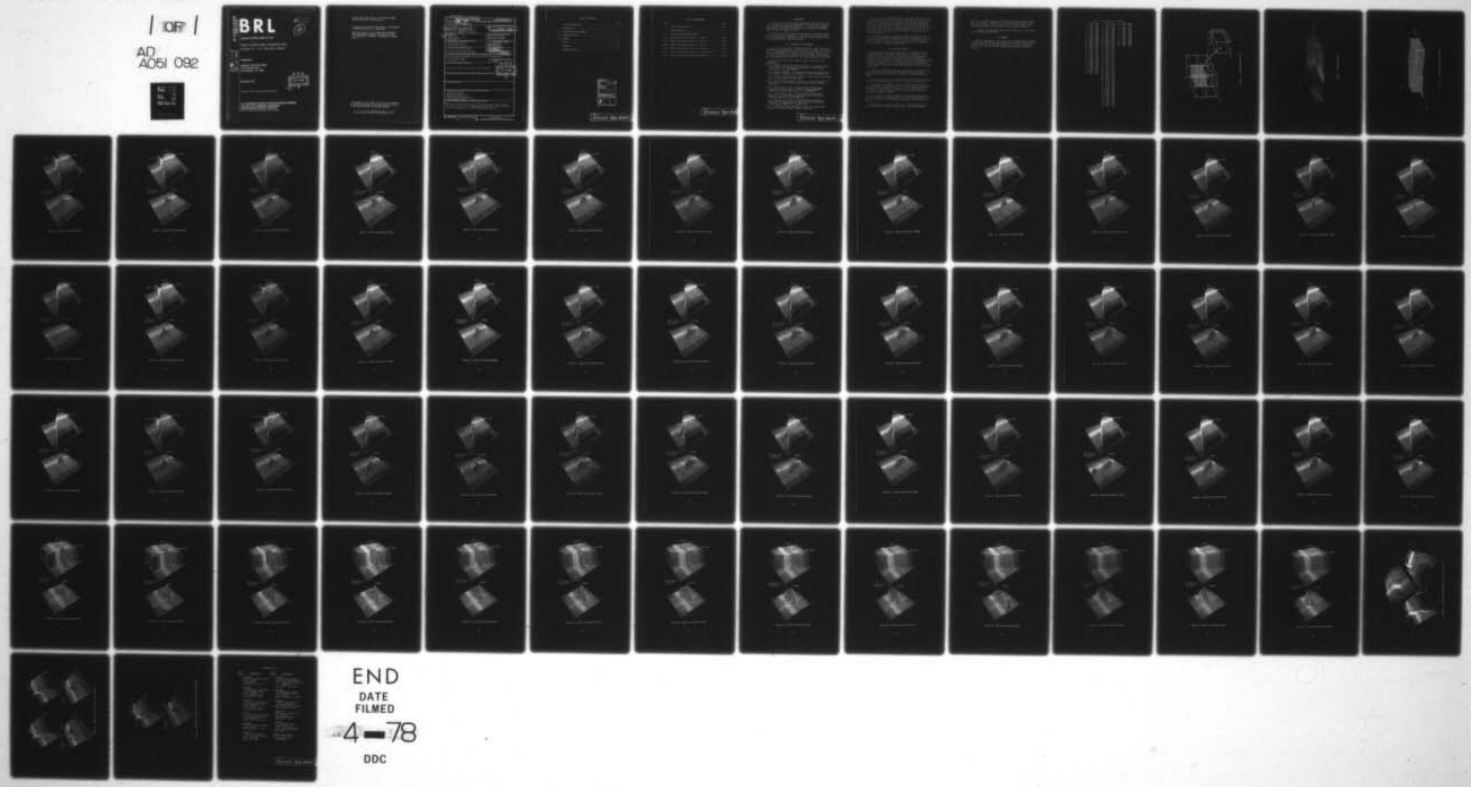

END
DATE
FILMED
4-78
DDC

per telecon w/ Foust 2-27-78 sent to DDC in Dec?

BRL

AD

12
B.S.

CONTRACT REPORT ARBRL-CR-356

THREE-DIMENSIONAL COMPUTATIONS, VOLUME IV: 77.5° OBLIQUE IMPACT

Prepared by

Computer Code Consultants
527 Glencrest Drive
Solana Beach, CA 92075

December 1977

USA ARMAMENT RESEARCH AND DEVELOPMENT COMMAND
USA BALLISTIC RESEARCH LABORATORY
ABERDEEN PROVING GROUND, MARYLAND

Destroy this report when it is no longer needed.
Do not return it to the originator.

Secondary distribution of this report by originating or sponsoring activity is prohibited.

Additional copies of this report may be obtained from the National Technical Information Service, U.S. Department of Commerce, Springfield, Virginia 22161.

The findings in this report are not to be construed as an official Department of the Army position, unless so designated by other authorized documents.

The use of trade names or manufacturers' names in this report does not constitute indorsement of any commercial product.

UNCLASSIFIED

SECURITY CLASSIFICATION OF THIS PAGE (When Data Entered)

REPORT DOCUMENTATION PAGE

READ INSTRUCTIONS BEFORE COMPLETING FORM

1. REPORT NUMBER: CONTRACT REPORT ARBRL-CR-356

2. GOVT ACCESSION NO.

3. RECIPIENT'S CATALOG NUMBER

4. TITLE (and Subtitle): THREE-DIMENSIONAL COMPUTATIONS, VOLUME IV: 77.5° OBLIQUE IMPACT

5. TYPE OF REPORT & PERIOD COVERED: Final rept. Apr 1976-Apr 1977

6. PERFORMING ORG. REPORT NUMBER

7. AUTHOR(s): W. Johnson, V. Kucher (BRL)

8. CONTRACT OR GRANT NUMBER(s): DAAD05-76-C-0755

9. PERFORMING ORGANIZATION NAME AND ADDRESS
Computer Code Consultants
527 Glencrest Drive
Solana Beach, CA 92075

10. PROGRAM ELEMENT, PROJECT, TASK AREA & WORK UNIT NUMBERS: 1W161102A33H

11. CONTROLLING OFFICE NAME AND ADDRESS
USA Ballistic Research Laboratory
Aberdeen Proving Ground, MD 21005

12. REPORT DATE: DEC 1977

13. NUMBER OF PAGES: 73 (12) 73p.

14. MONITORING AGENCY NAME & ADDRESS (if different from Controlling Office)
US Army Materiel Development & Readiness Command
5001 Eisenhower Avenue
Alexandria, VA 22333

15. SECURITY CLASS. (of this report): UNCLASSIFIED

15a. DECLASSIFICATION/DOWNGRADING SCHEDULE

16. DISTRIBUTION STATEMENT (of this Report)

Approved for public release; distribution unlimited.

17. DISTRIBUTION STATEMENT (of the abstract entered in Block 20, if different from Report)

18. SUPPLEMENTARY NOTES

19. KEY WORDS (Continue on reverse side if necessary and identify by block number)
Penetration mechanics
Hypervelocity impact
Hydrodynamic computer code
Three-dimensional computer code
Eulerian computer code

20. ABSTRACT (Continue on reverse side if necessary and identify by block number)

Numerical calculations were made in 1975 of four oblique impact problems: 30°, 45°, 60°, and 77.5°. A graphical display of the results of the 77.5° impact of a copper jet on a steel target are presented.

DD FORM 1 JAN 73 1473 EDITION OF 1 NOV 65 IS OBSOLETE

391 758 JOB

UNCLASSIFIED

SECURITY CLASSIFICATION OF THIS PAGE (When Data Entered)

TABLE OF CONTENTS

LIST OF ILLUSTRATIONS

I. INTRODUCTION

A series of four oblique impact computations (30°, 45°, 60°, and 77.5°) involving a copper jet impacting a steel plate were completed in 1975 for the Ballistic Research Laboratory.[1] This work was performed using TRIDORF[2] and DORF[3,4] and ancillary programs CUBIT[3] and ADJUST[4] under Contract No. DAAD05-75-C-0738.

The effort for 1976 has been directed towards a graphical display of the data from these computations. The four oblique impacts in the series are presented in sequential volumes[5,6,7] with the results of the 77.5° obliquity impact being reported here.

II. DESCRIPTION OF THE PROBLEM

The 77.5° oblique impact computation involved a copper jet with a 0.7086-mm radius impacting on a 12.7-mm thick steel target. The obliquity angle is measured between the normal to the target and the axis of the jet. Since TRIDORF uses a retangular grid, the copper jet was treated as a bar with a square cross section of 1.256-mm width, thus preserving the cross-sectional area of the jet. The impact velocity was 7.55 km/s.

The Tillotson[8] form of the equation of state was used for the computations.

---

1. W. E. Johnson, "Three-Dimensional Computations on Penetrator-Target Interactions," Ballistic Research Laboratory Contractor Report No. 338, May 1977. (AD #A041058)

2. W. E. Johnson, "TRIDORF - A Two-Material Version of the TRIOIL Code with Strength," Computer Code Consultants, CCC-976, September 1976.

3. W. E. Johnson, "Code Correlation Study," Air Force Weapons Laboratory Report No. AFWL-TR-70-144, April 1971.

4. W. E. Johnson, "Development and Application of Computer Programs to Hypervelocity Impact," Systems, Science and Software, 3SR-749, July 1971.

5. W. E. Johnson and V. Kucher, "Three-Dimensional Computations, Volume I: 30° Oblique Impact", Ballistic Research Laboratory Contractor Report No. 344, July 1977. (AD #A043295)

6. W. E. Johnson and V. Kucher, "Three-Dimensional Computations, Volume II: 45° Oblique Impact", Ballistic Research Laboratory Contractor Report.No. 354, November 1977.

7. W. E. Johnson and V. Kucher, "Three-Dimensional Computations, Volume III: 60° Oblique Impact", Ballistic Research Laboratory Contract Report ARBRL-CR-355, December 1977.

8. J. H. Tillotson, "Metallic Equations of State for Hypervelocity Impact," Gulf General Atomic, GA-3216, July 1962.

A view of a three-dimensional grid is shown in Figure 1. Each cell is identified by the coordinates (I,J,K), which number the cells in the x,y,z-directions, respectively. The overall size of the computational grid was x = 19.884 mm by y = 55.596 mm by z = 8.367 mm. The maximum number of cells in the x-direction was I = 36, in the y-direction, J = 60, and in the z-direction, K = 15. The total number of cells in the grid was 32,400. Table I presents the dimensions of the cells, DX, DY, and DZ, and the grid coordinates as shown in Figure 1. These data are displayed in Figure 2.

The xy-plane was used as a plane of symmetry through the bar in order to keep the number of computational cells at a minimum. Since the width of the bar was four cells, the bar was two cells wide from the plane of symmetry. Figure 3 shows the penetrator-target configuration as it is located in the computational grid.

III. GRAPHICAL RESULTS

The numerical output of the computations is presented as density and pressure fields. The density and pressure are plotted on a two-dimensional spatial plane having the coordinates corresponding to the centers of cells. The fields are plotted such that a cell-number coordinate is held constant. For example, K may be constant meaning that the density or pressure is being presented for the cells between two z-planes bounding the K-cells. These bounding planes will be indicated in each figure. Figures 2 and 3 should be useful for orienting oneself in the grid.

The density scale for the density field plots can be realized from the initial density of the jet and the target, 8.9 and 7.8 Mg/m^3, respectively. The density scale is the same in all the density field plots.

The pressure scale is not the same in all the pressure field plots; therefore, the maximum pressure, Pmax, is indicated on each figure.

The first set of figures, Figures 4-18, shows the density and pressure fields at a constant time of 1.55 μs for various K-slabs which are numbered from the plane of symmetry. The jet appears distinct only when K = 1 and K = 2 since, initially, the jet was two cells in width from the plane of symmetry.

The second set of figures, Figures 19-32, shows the density and pressure fields at a constant time of 2.23 μs for various K-slabs. Data for K = 12 could not be recovered from the magnetic output tapes for plotting.

The third set of figures, Figures 33-45, shows the density and pressure fields at a constant time of 2.65 μs for various K-slabs.

Data for K = 3 and K = 6 could not be recovered from the magnetic output tapes for plotting. Another view of the corresponding figures in the third set of figures is shown in Figures 46-58. Also, three views of of the density field at 2.65 μs for K = 1 are shown in Figure 59.

A comparison of the density and pressure fields at K = 1 for various times is shown in Figures 60-61.

IV. SUMMARY

Numerical computations were made in 1975 of oblique impact problems. A graphical display of the results of the 77.5° impact of a copper jet on a steel target are presented for future analysis. The results for the 30°, 45°, 60°, and 77.5° oblique impacts are presented in sequential volumes.

Table I. Grid Coordinates and Cell Dimensions

I	x (mm)	DX (mm)	J	y (mm)	DY (mm)	K	z (mm)	DZ (mm)
1	2.172	2.172	1	6.379	6.379	1	0.314	0.314
2	3.672	1.500	2	9.874	3.495	2	0.628	0.314
3	4.672	1.000	3	11.674	1.800	3	0.942	0.314
4	5.372	0.700	4	13.274	1.600	4	1.256	0.314
5	5.872	0.500	5	14.674	1.400	5	1.601	0.345
6	6.372	0.500	6	15.874	1.200	6	1.981	0.380
7	6.872	0.500	7	16.874	1.000	7	2.399	0.418
8	7.372	0.500	8	17.674	0.800	8	2.859	0.460
9	7.872	0.500	9	18.274	0.600	9	3.365	0.506
10	8.372	0.500	10	18.774	0.500	10	3.921	0.556
11	8.872	0.500	11	19.174	0.400	11	4.540	0.619
12	9.372	0.500	12	19.488	0.314	12	5.213	0.673
13	9.872	0.500	13	19.802	0.314	13	5.953	0.740
14	10.372	0.500	14	20.116	0.314	14	6.767	0.814
15	10.872	0.500	15	20.430	0.314	15	8.367	1.600
16	11.372	0.500	16	20.744	0.314			
17	11.686	0.314	17	21.058	0.314			
18	12.000	0.314	18	21.372	0.314			
19	12.314	0.314	19	21.686	0.314			
20	12.628	0.314	20	22.000	0.314			
21	12.942	0.314	21	22.314	0.314			
22	13.256	0.314	22	22.628	0.314			
23	13.570	0.314	23	22.942	0.314			
24	13.884	0.314	24	23.256	0.314			
25	14.384	0.500	25	23.570	0.314			
26	14.884	0.500	26	23.884	0.314			
27	15.384	0.500	27	24.198	0.314			
28	15.884	0.500	28	24.512	0.314			
29	16.384	0.500	29	24.857	0.345			
30	16.884	0.500	30	25.237	0.380			
31	17.384	0.500	31	25.655	0.418			
32	17.884	0.500	32	26.115	0.460			
33	18.384	0.500	33	26.621	0.506			
34	18.884	0.500	34	27.177	0.556			
35	19.384	0.500	35	27.796	0.619			
36	19.884	0.500	36	28.596	0.800			
			37	29.396	0.800			
			38	30.196	0.800			
			39	30.996	0.800			
			40	31.796	0.800			
			41	32.596	0.800			
			42	33.396	0.800			
			43	34.196	0.800			
			44	34.996	0.800			
			45	35.796	0.800			
			46	36.596	0.800			
			47	37.396	0.800			
			48	38.196	0.800			
			49	38.996	0.800			
			50	39.796	0.800			
			51	40.596	0.800			
			52	41.396	0.800			
			53	42.196	0.800			
			54	42.996	0.800			
			55	43.796	0.800			
			56	44.596	0.800			
			57	45.396	0.800			
			58	46.196	0.800			
			59	49.396	3.200			
			60	52.596	3.200			

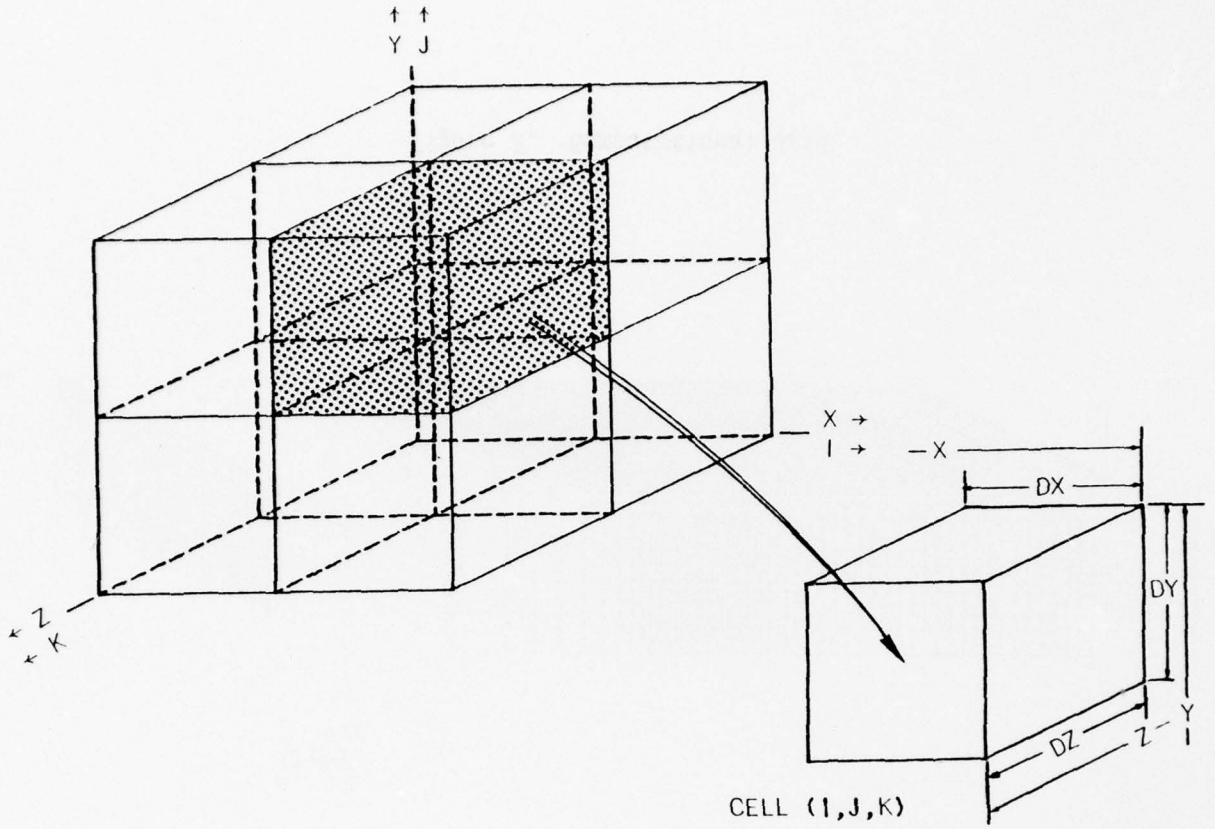

Figure 1. A Three-Dimensional Grid

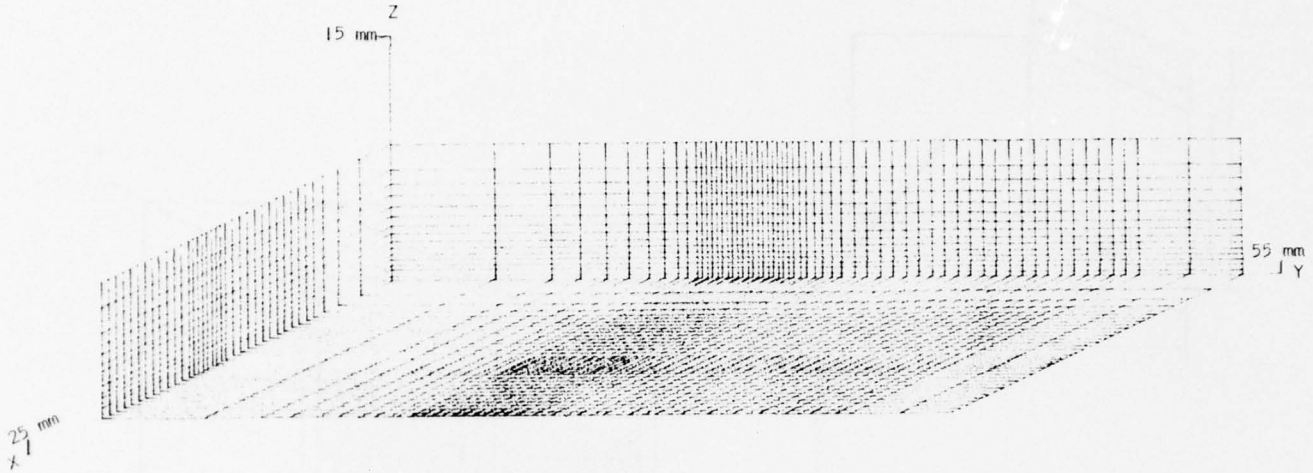

Figure 2. Computational Grid

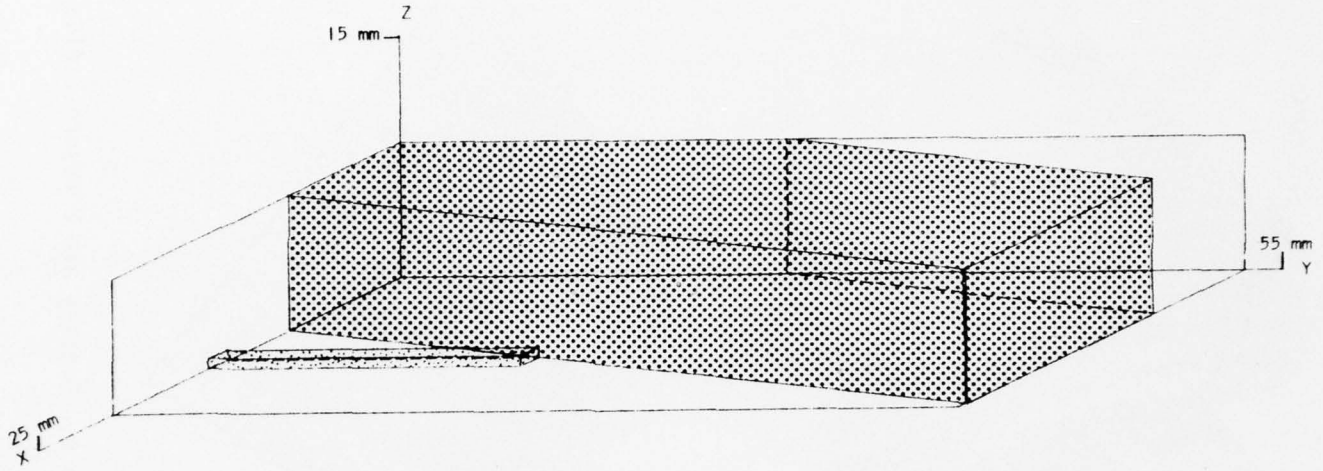

Figure 3. Penetrator-Target Configuration

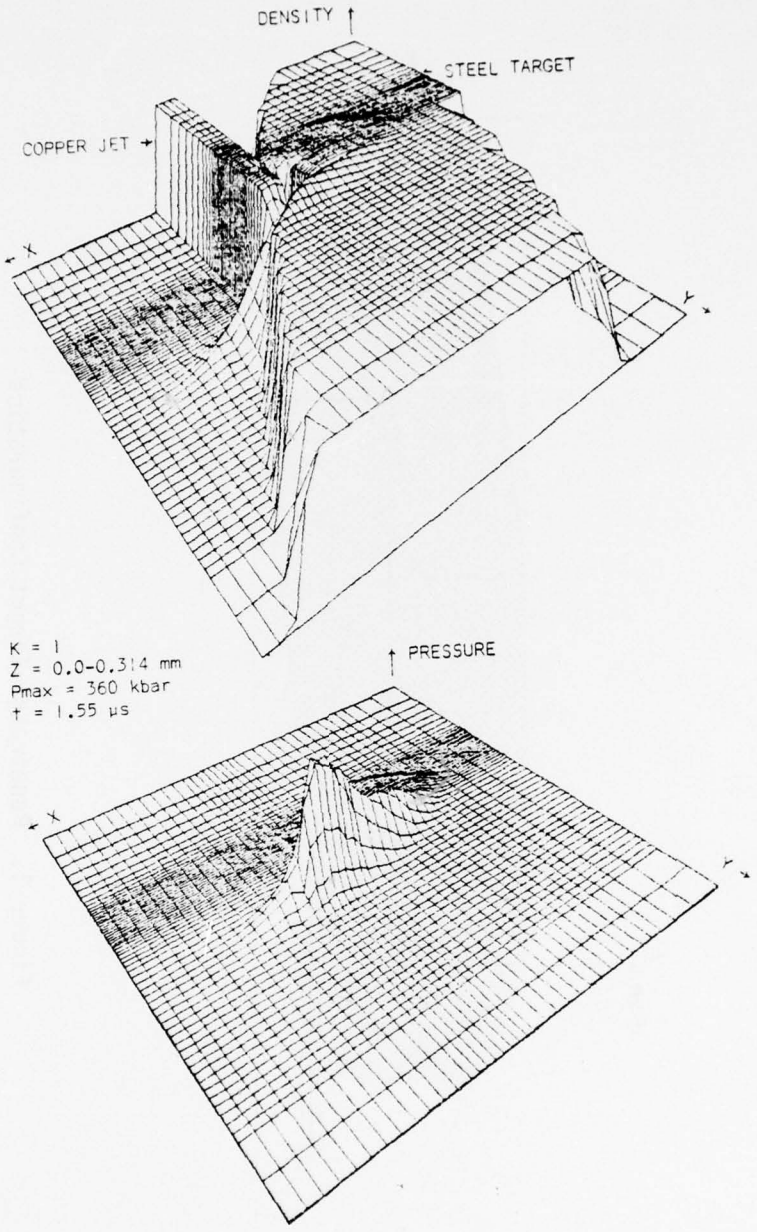

Figure 4. Density and Pressure Fields

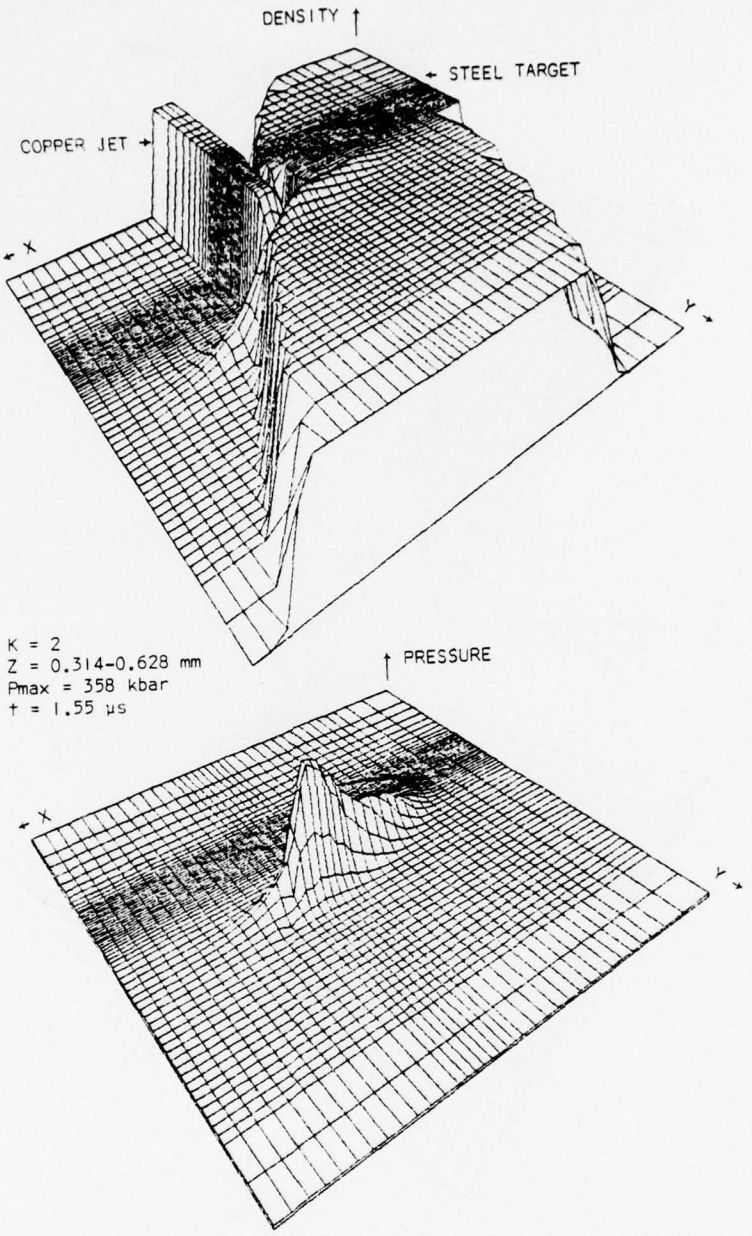

Figure 5. Density and Pressure Fields

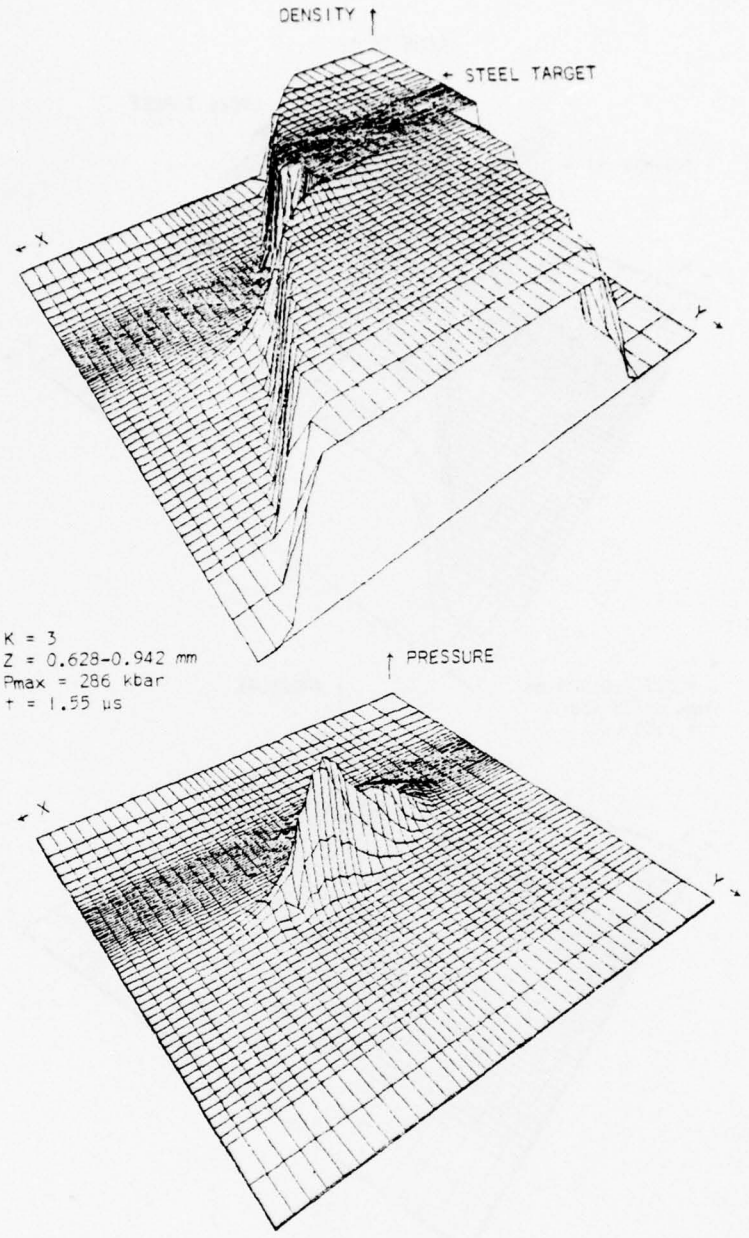

Figure 6. Density and Pressure Fields

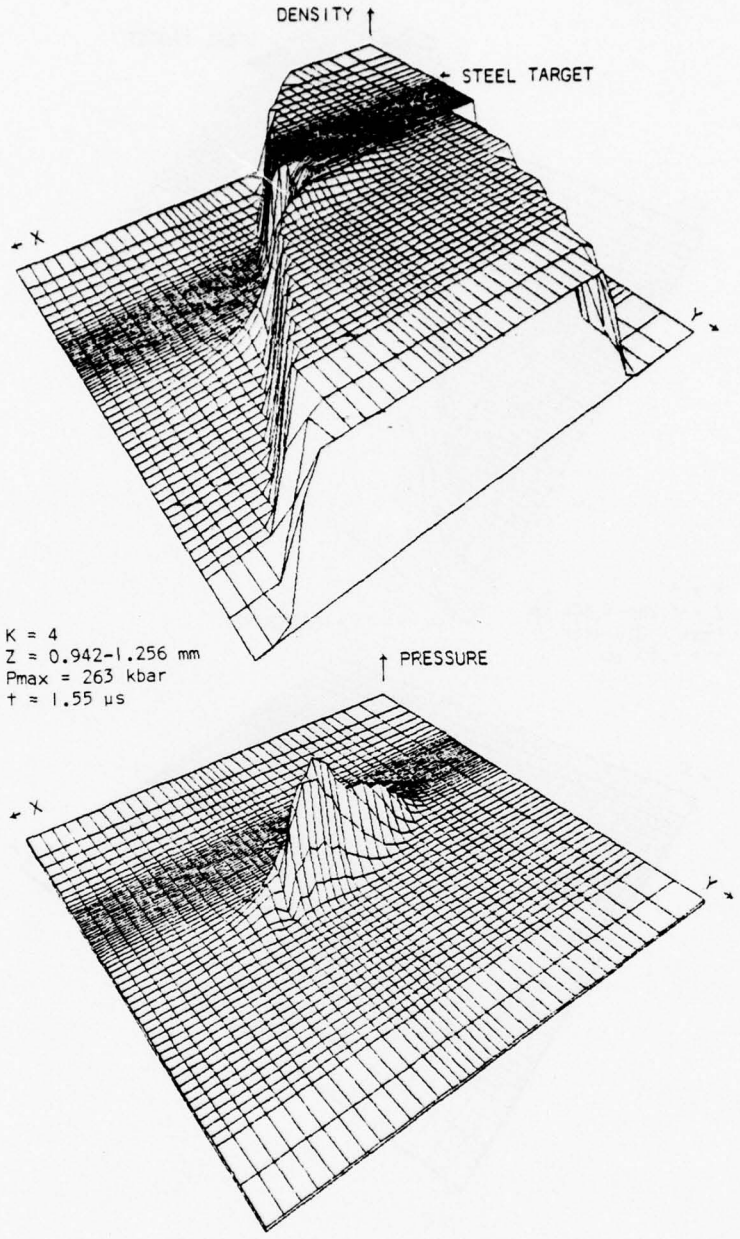

Figure 7. Density and Pressure Fields

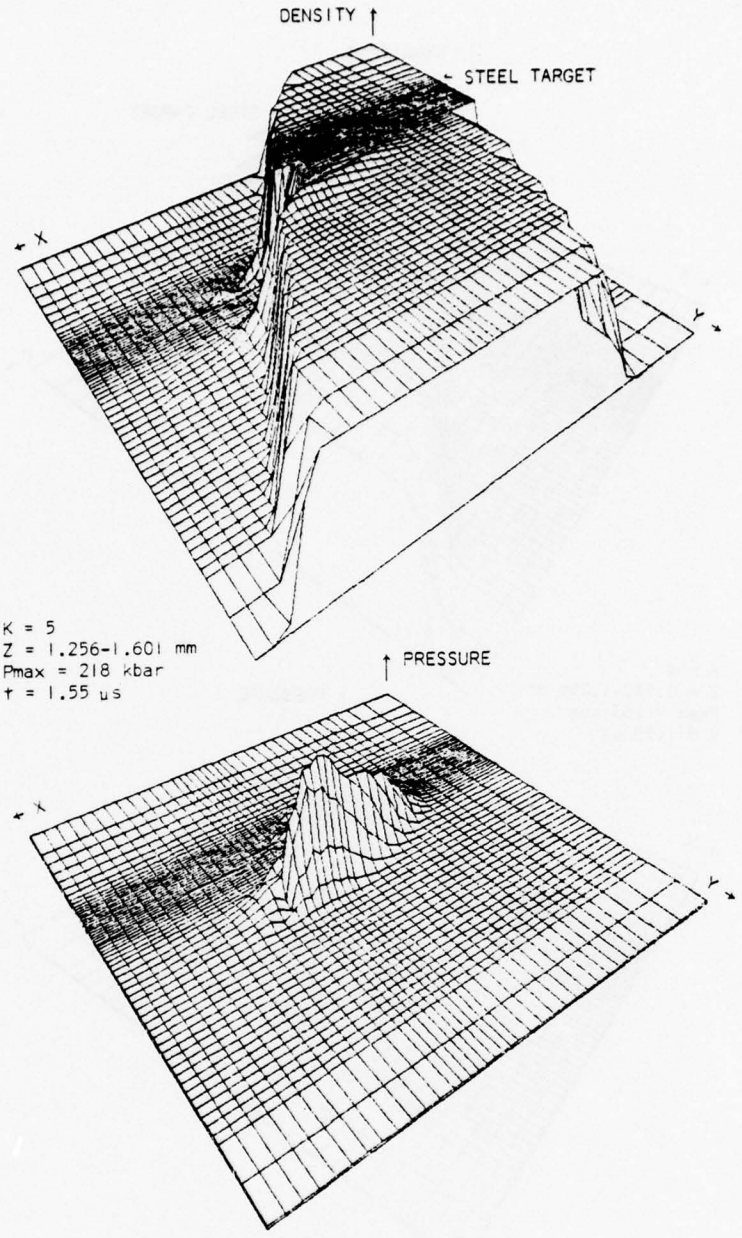

Figure 8. Density and Pressure Fields

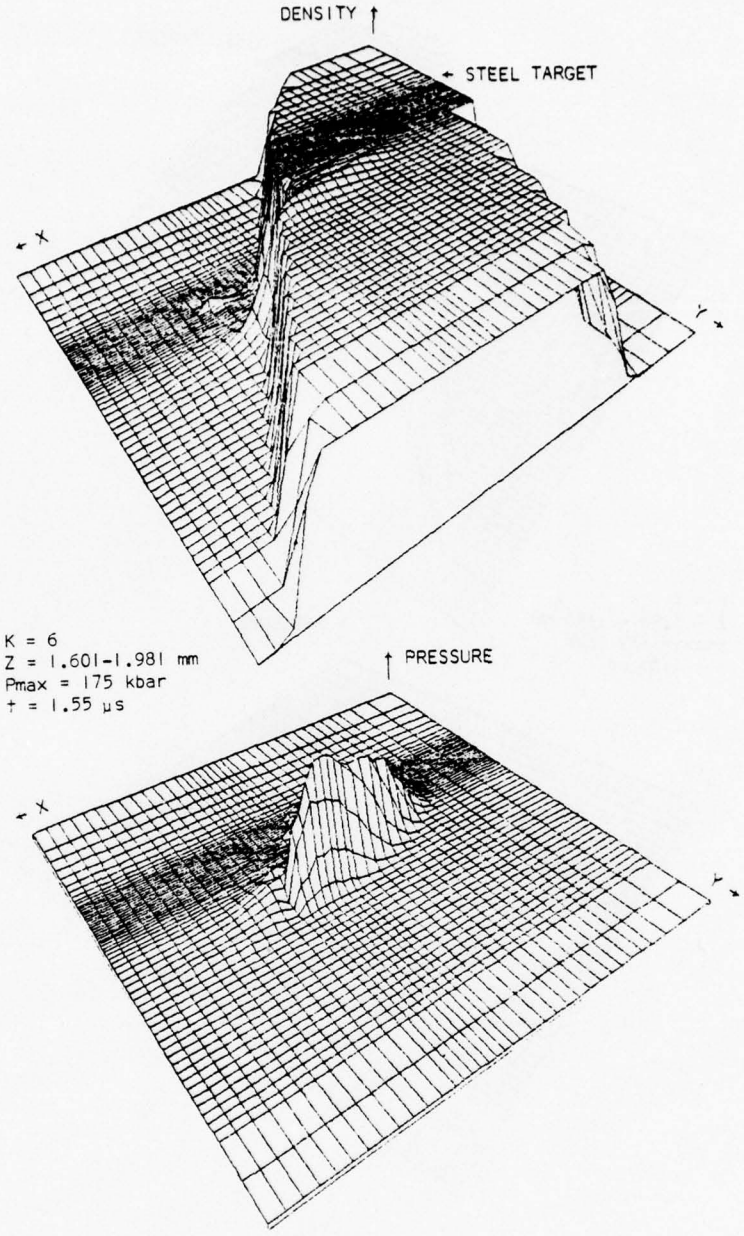

Figure 9. Density and Pressure Fields

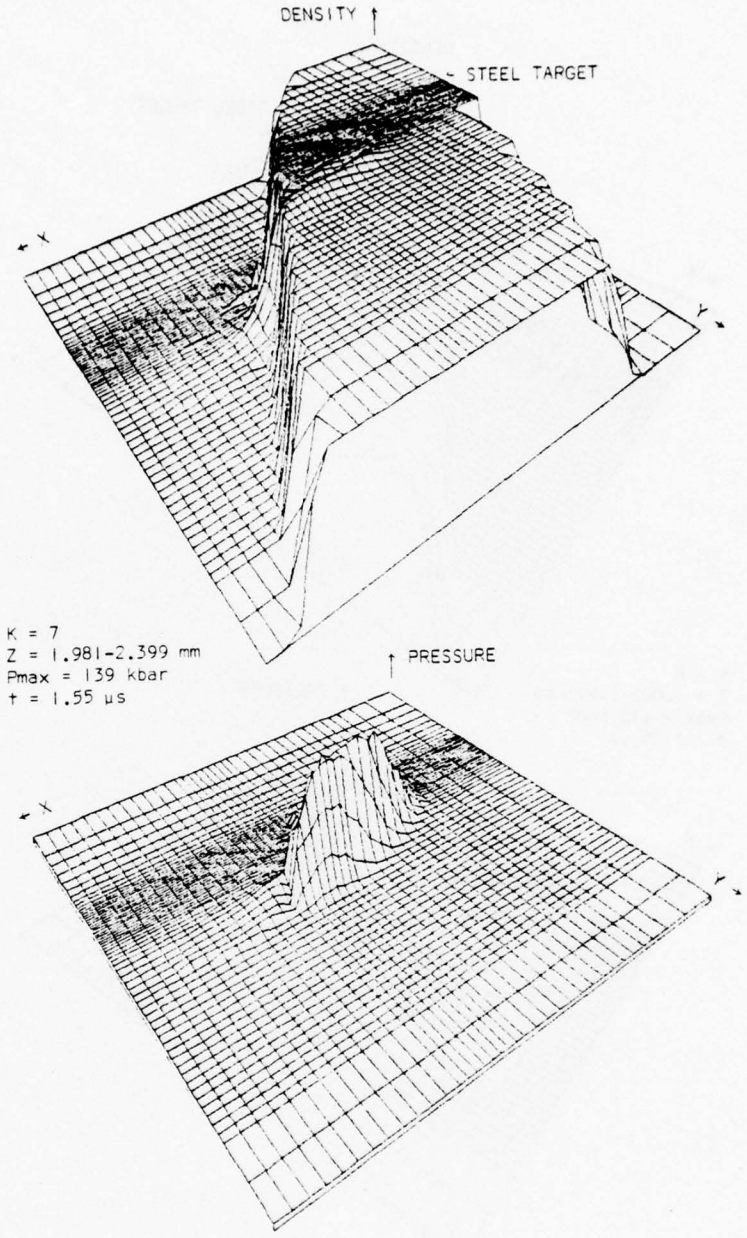

Figure 10. Density and Pressure Fields

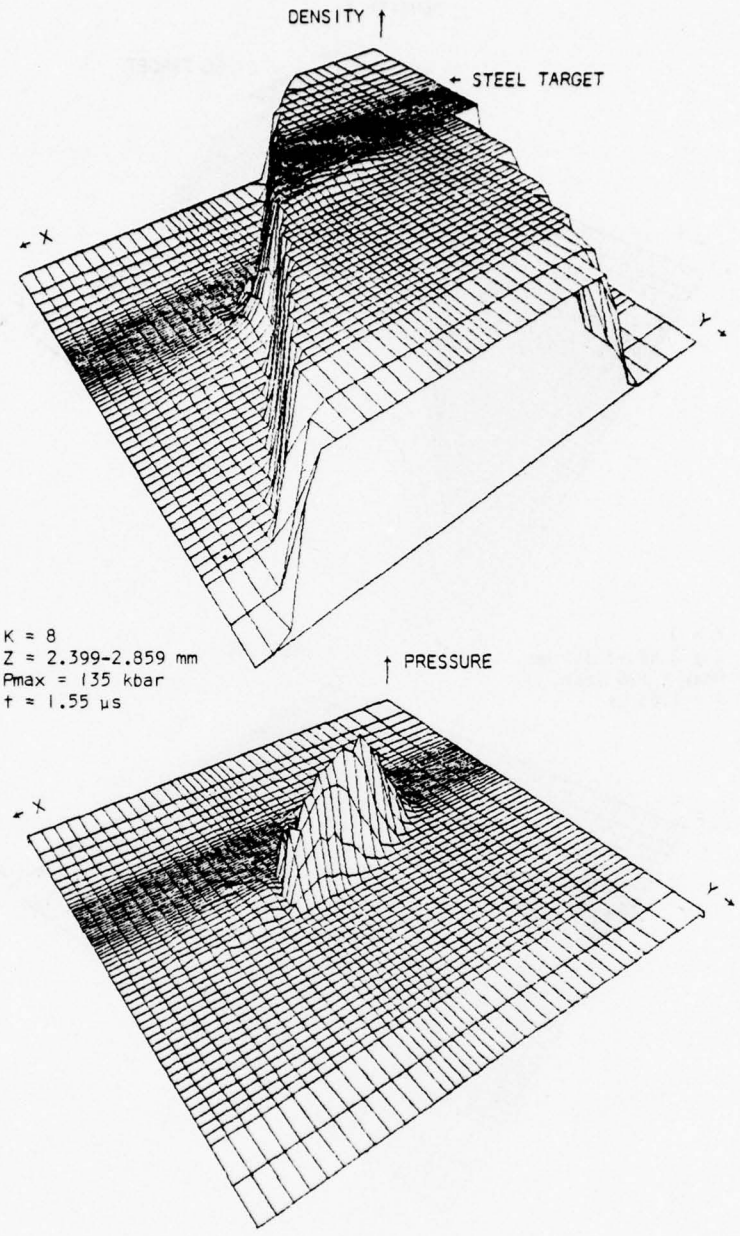

Figure 11. Density and Pressure Fields

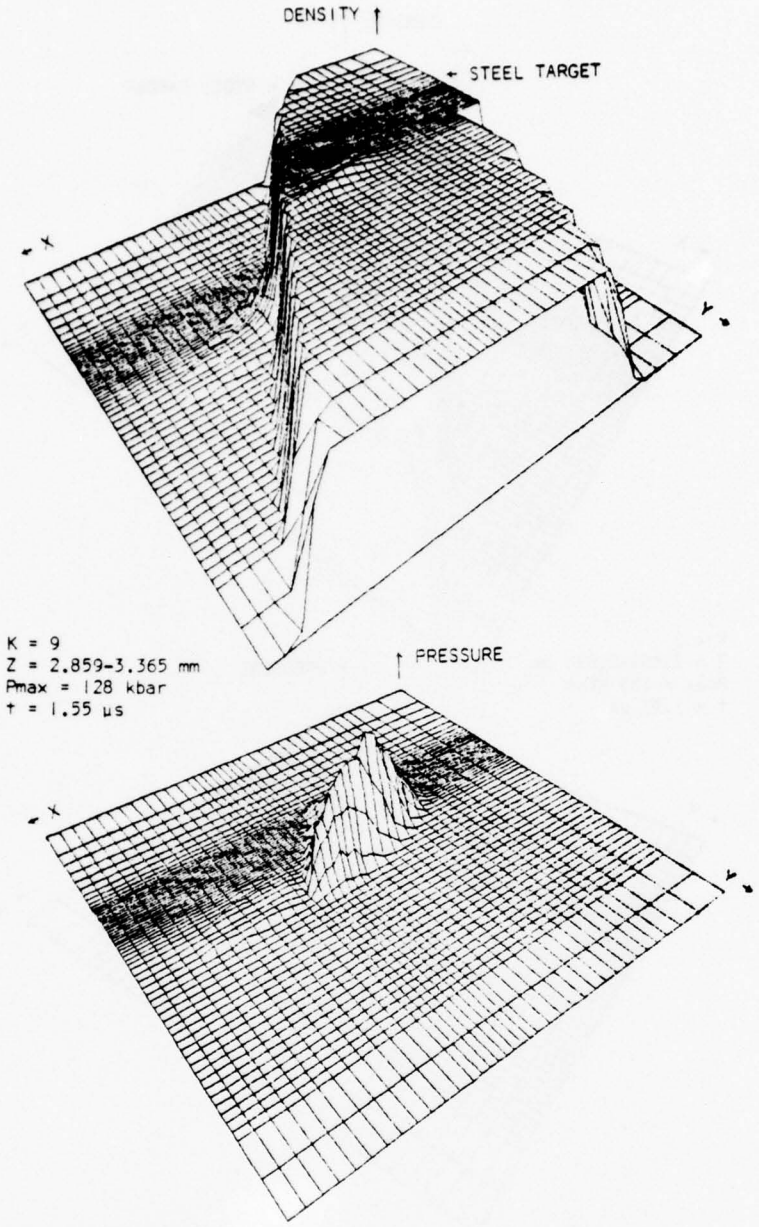

Figure 12. Density and Pressure Fields

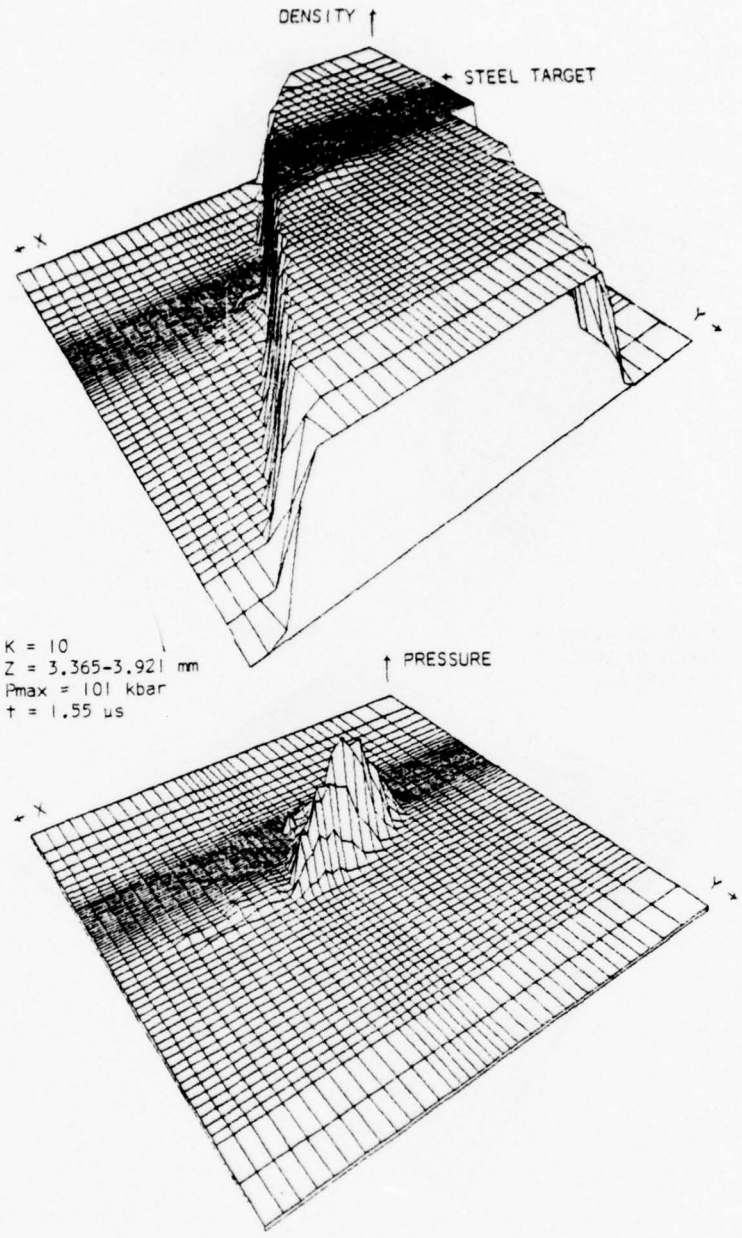

Figure 13. Density and Pressure Fields

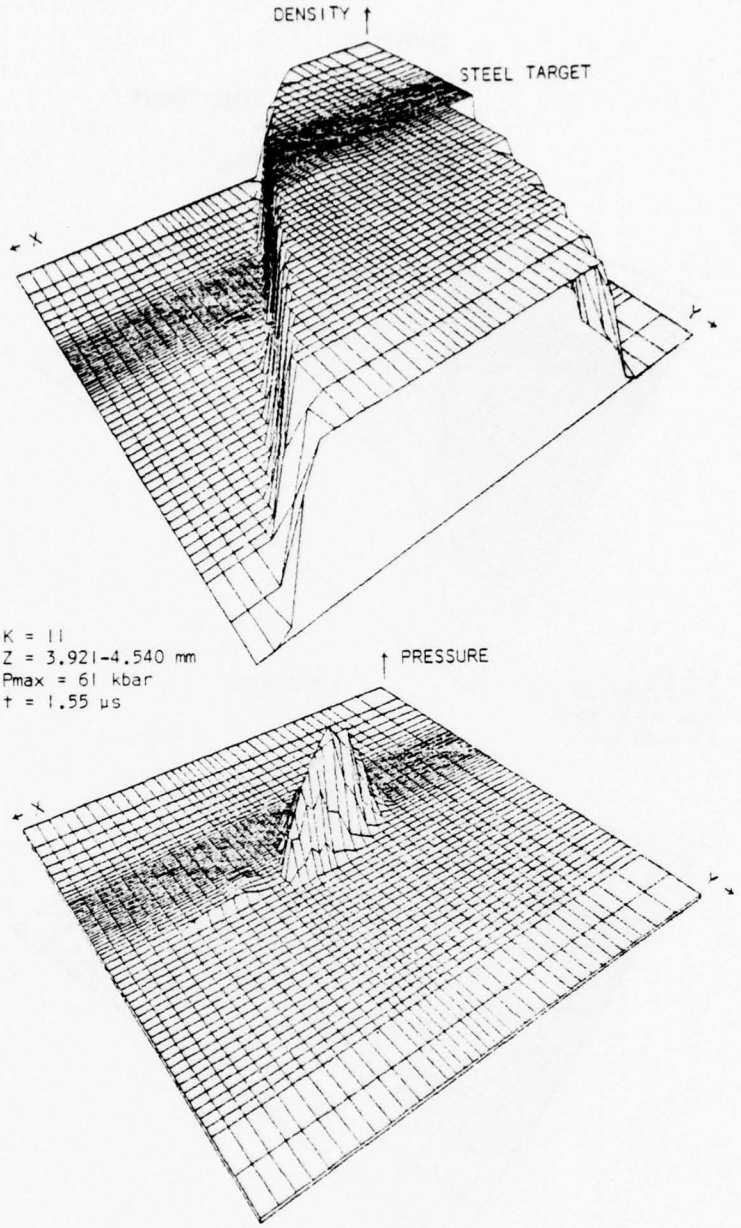

Figure 14. Density and Pressure Fields

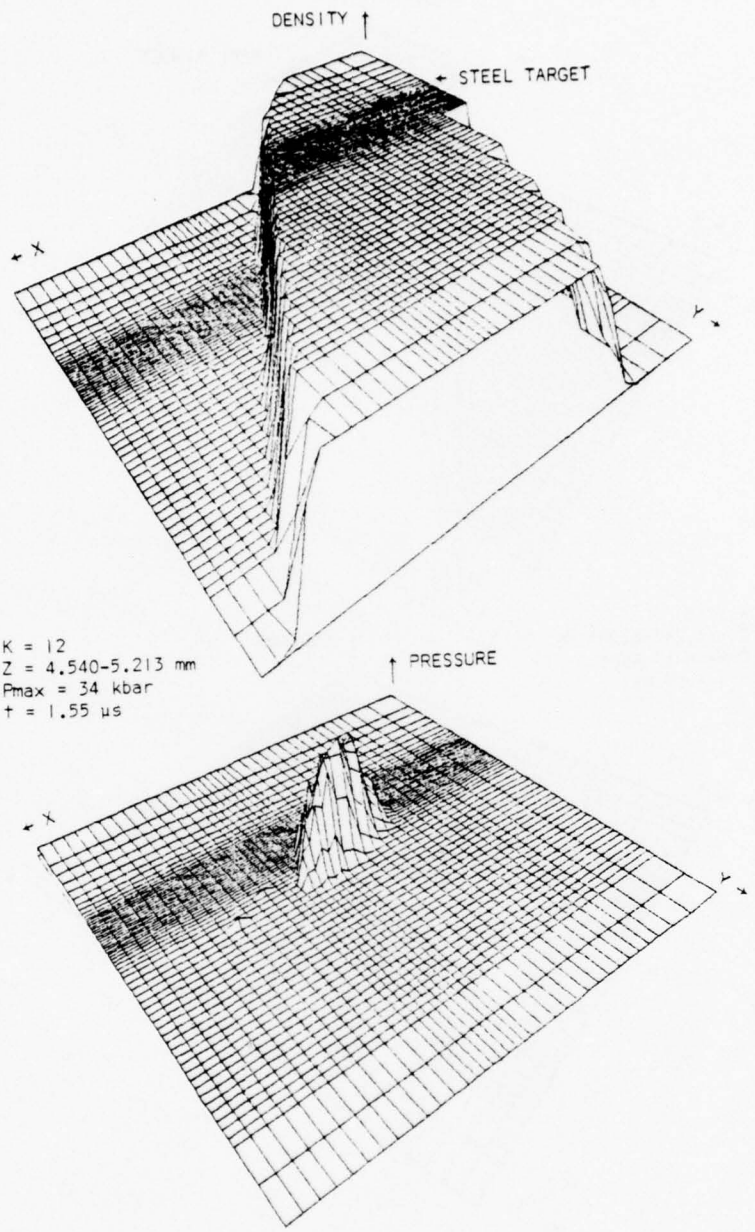

Figure 15. Density and Pressure Fields

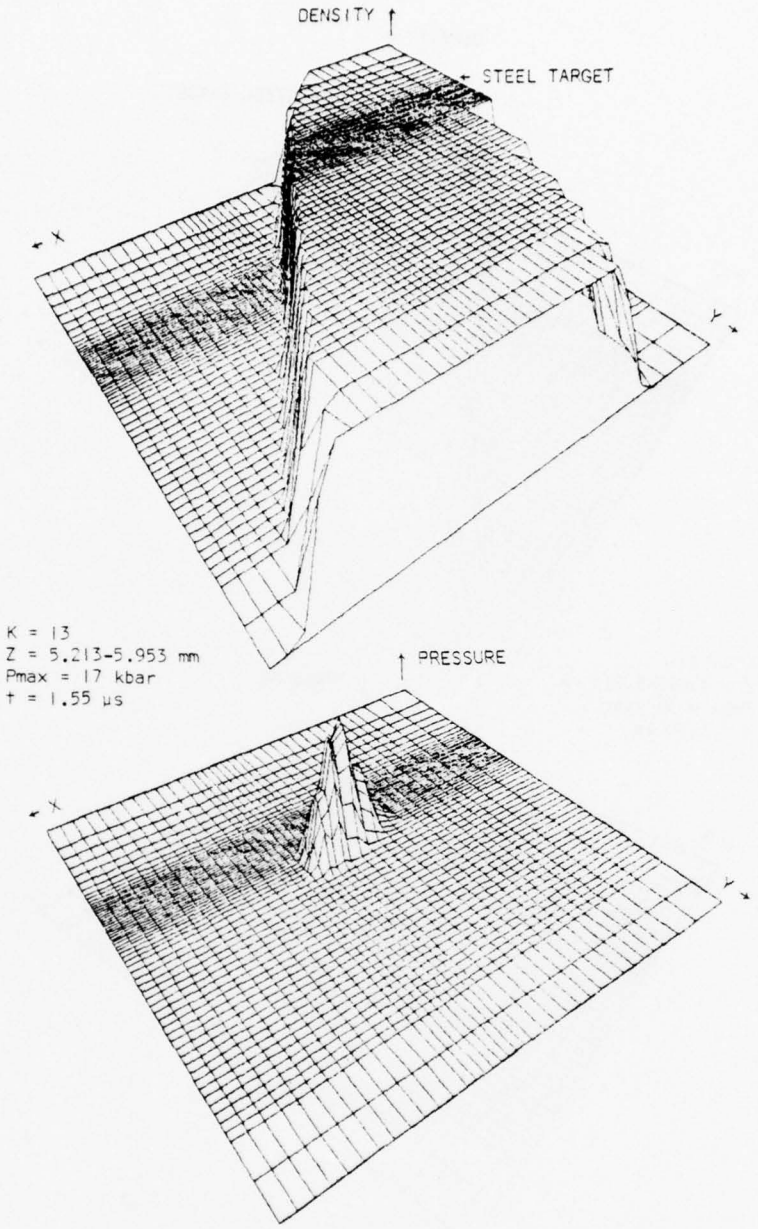

Figure 16. Density and Pressure Fields

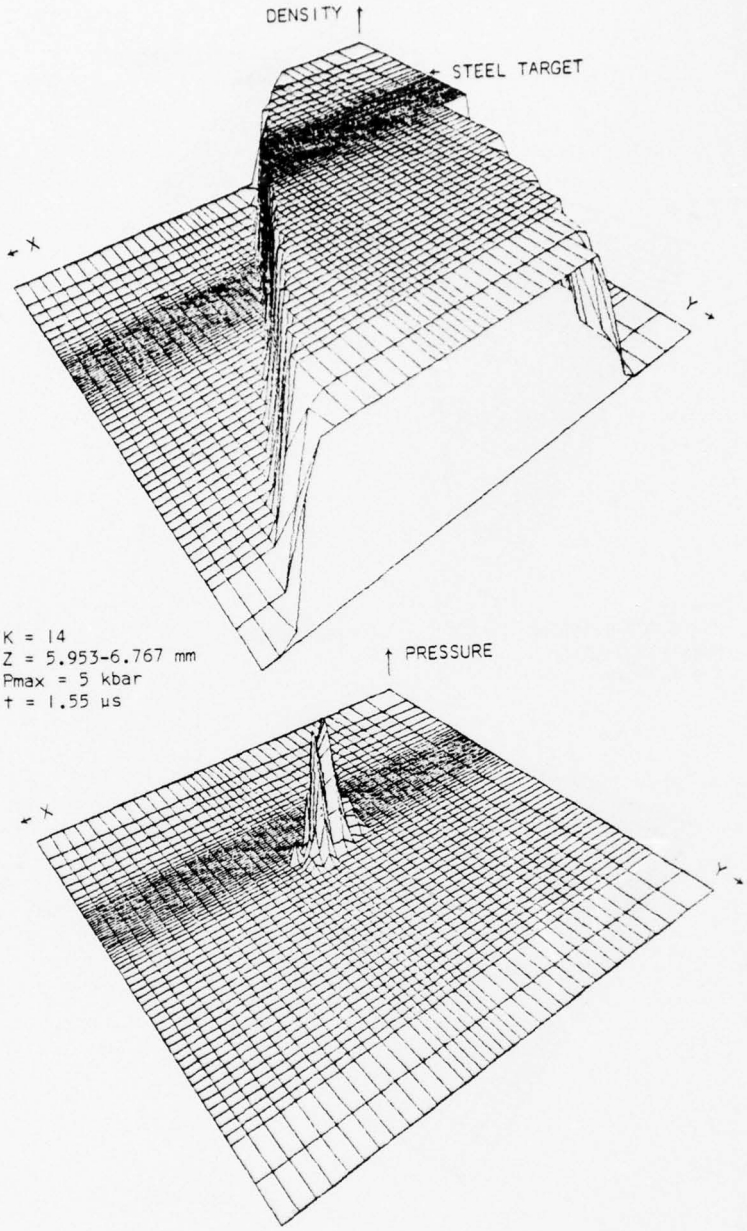

Figure 17. Density and Pressure Fields

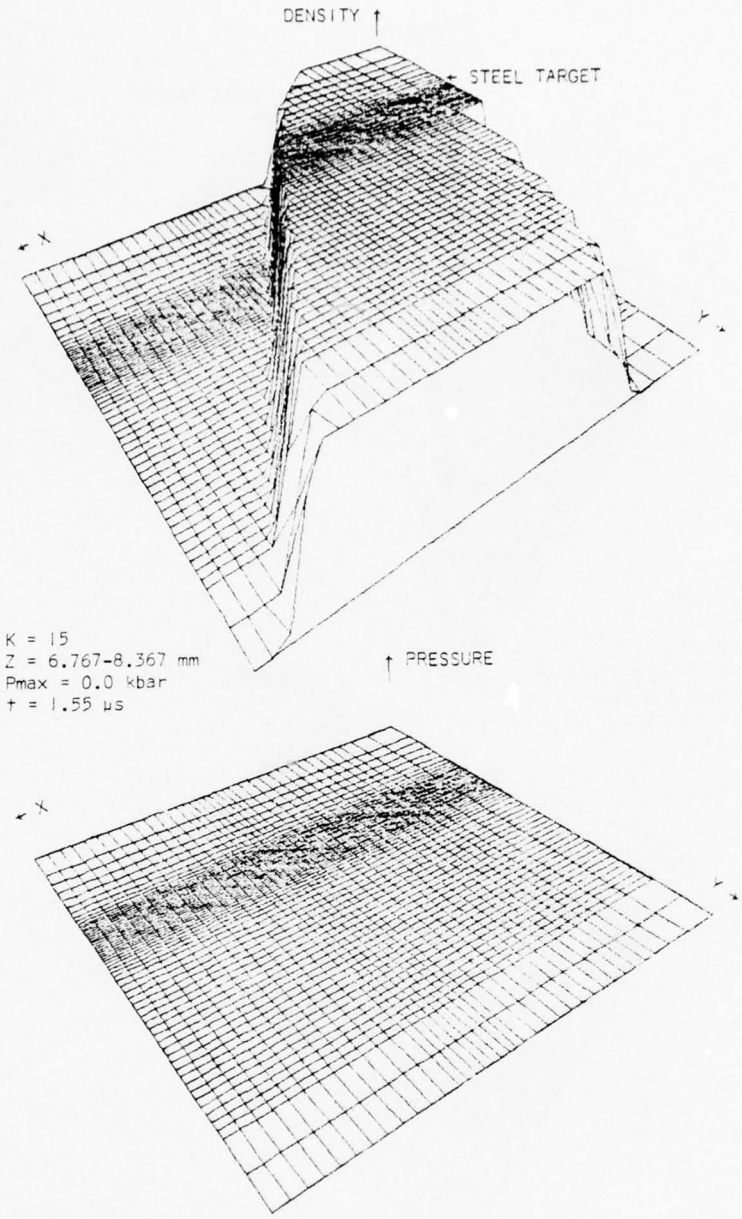

Figure 18. Density and Pressure Fields

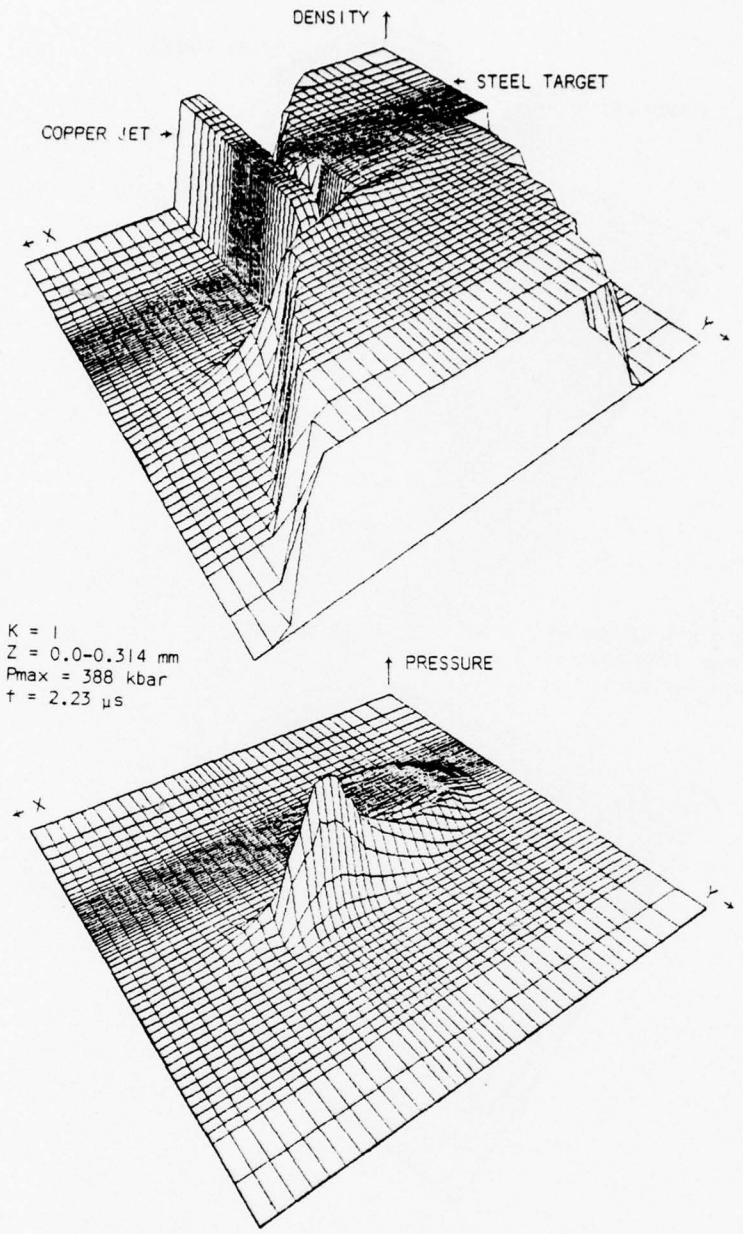

Figure 19. Density and Pressure Fields

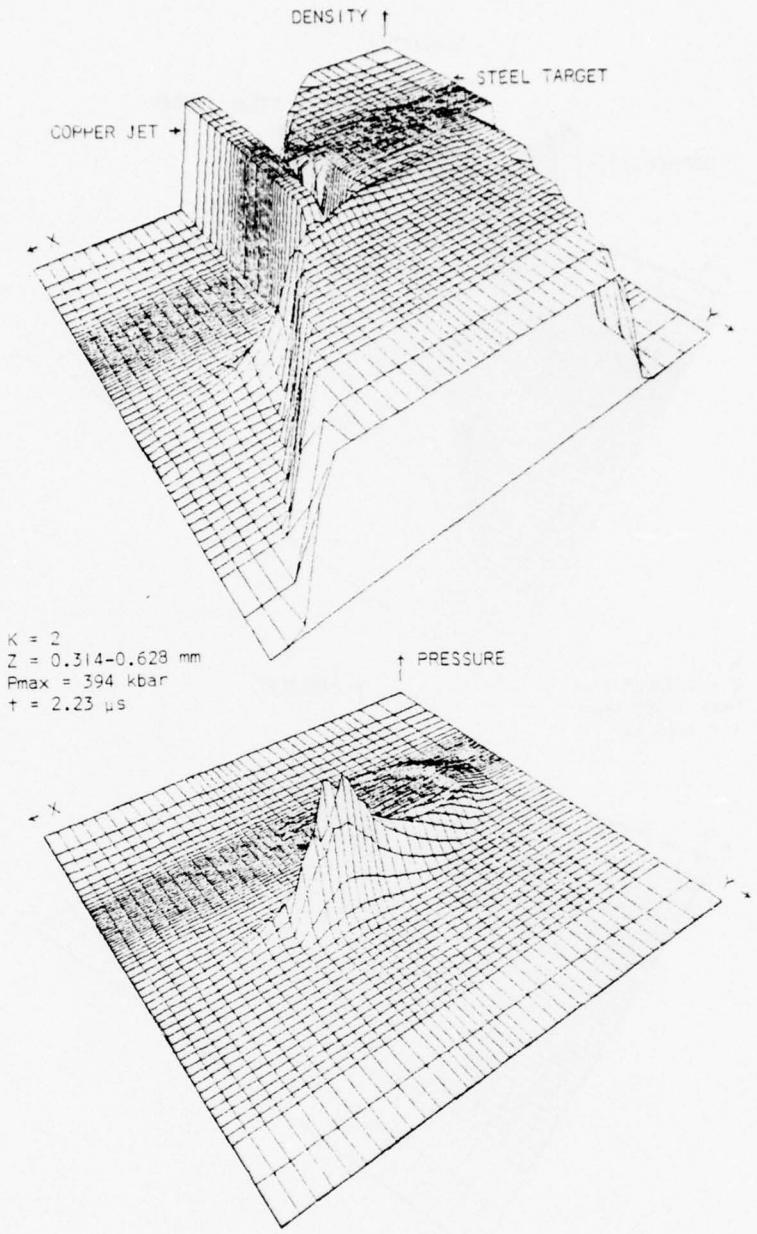

Figure 20. Density and Pressure Fields

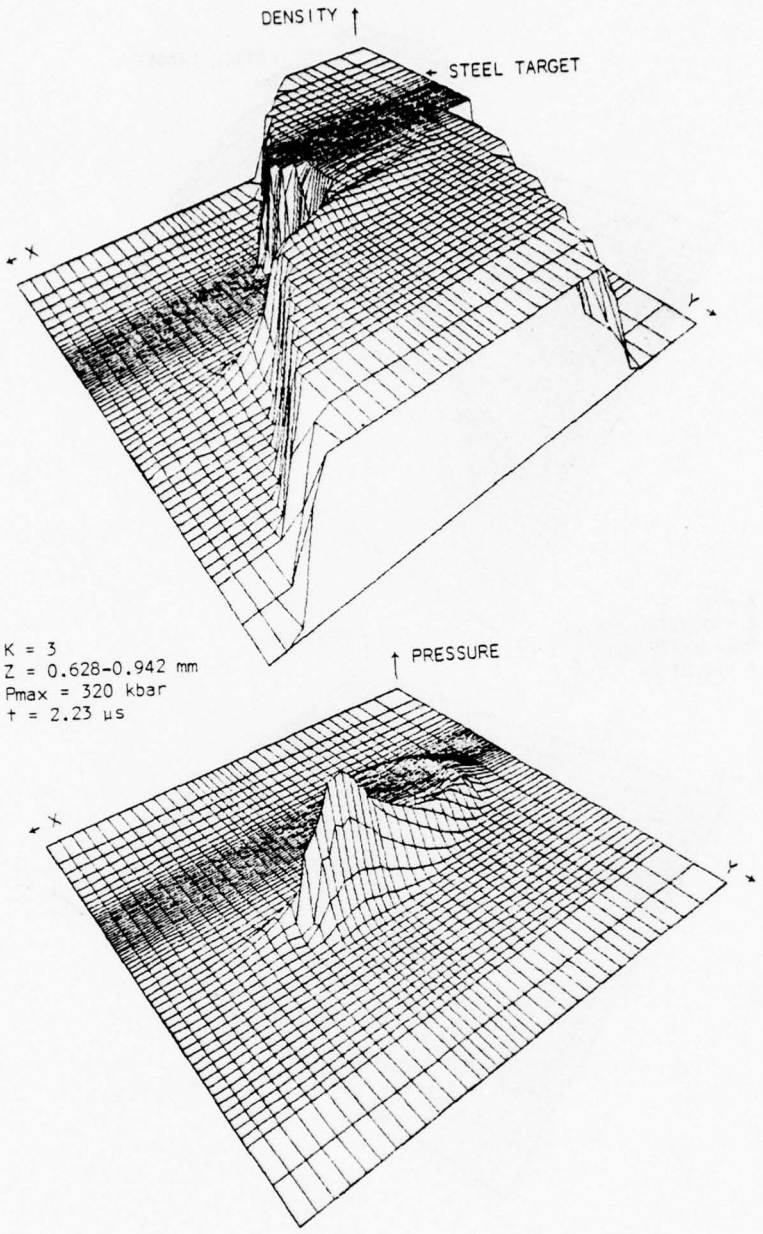

Figure 21. Density and Pressure Fields

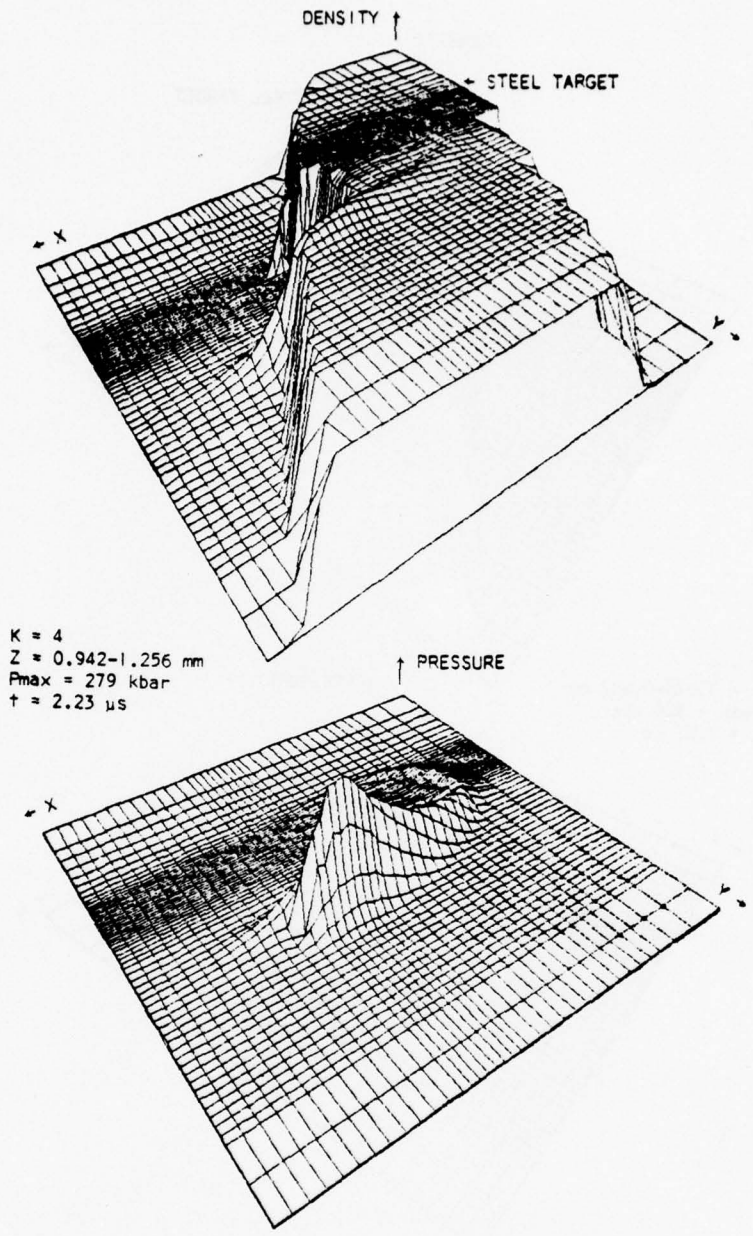

Figure 22. Density and Pressure Fields

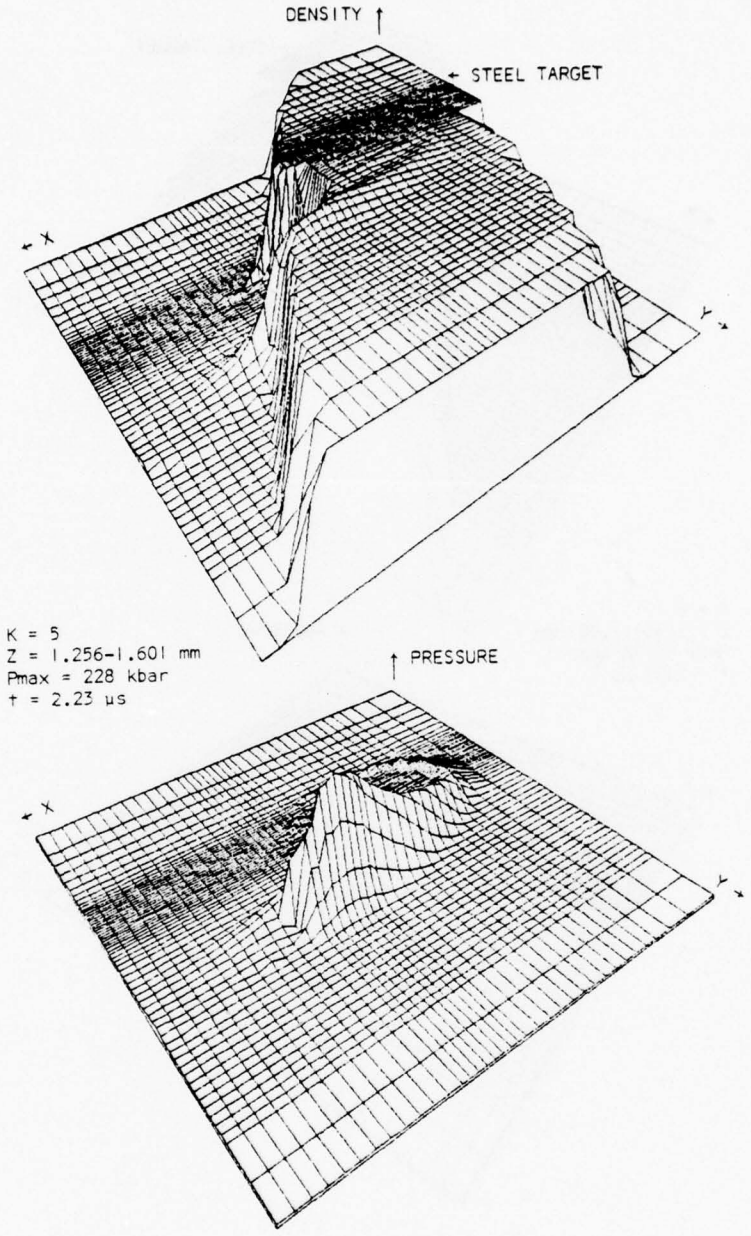

Figure 23. Density and Pressure Fields

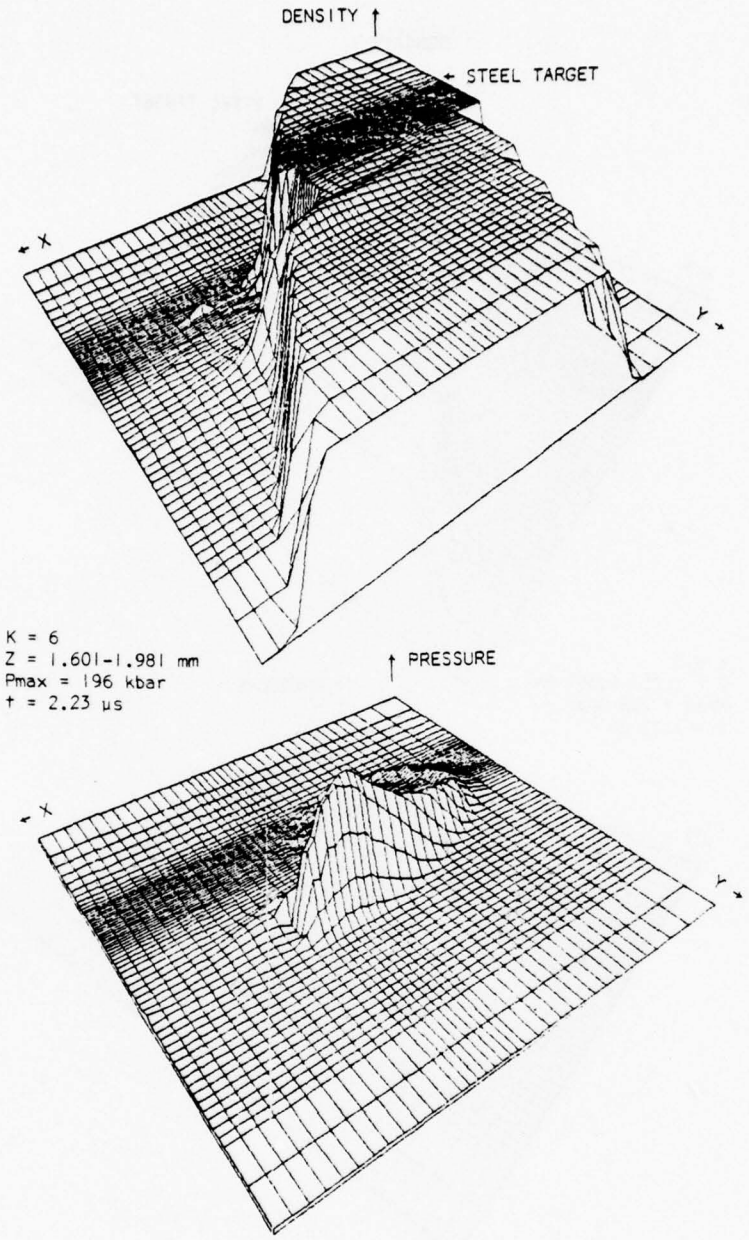

Figure 24. Density and Pressure Fields

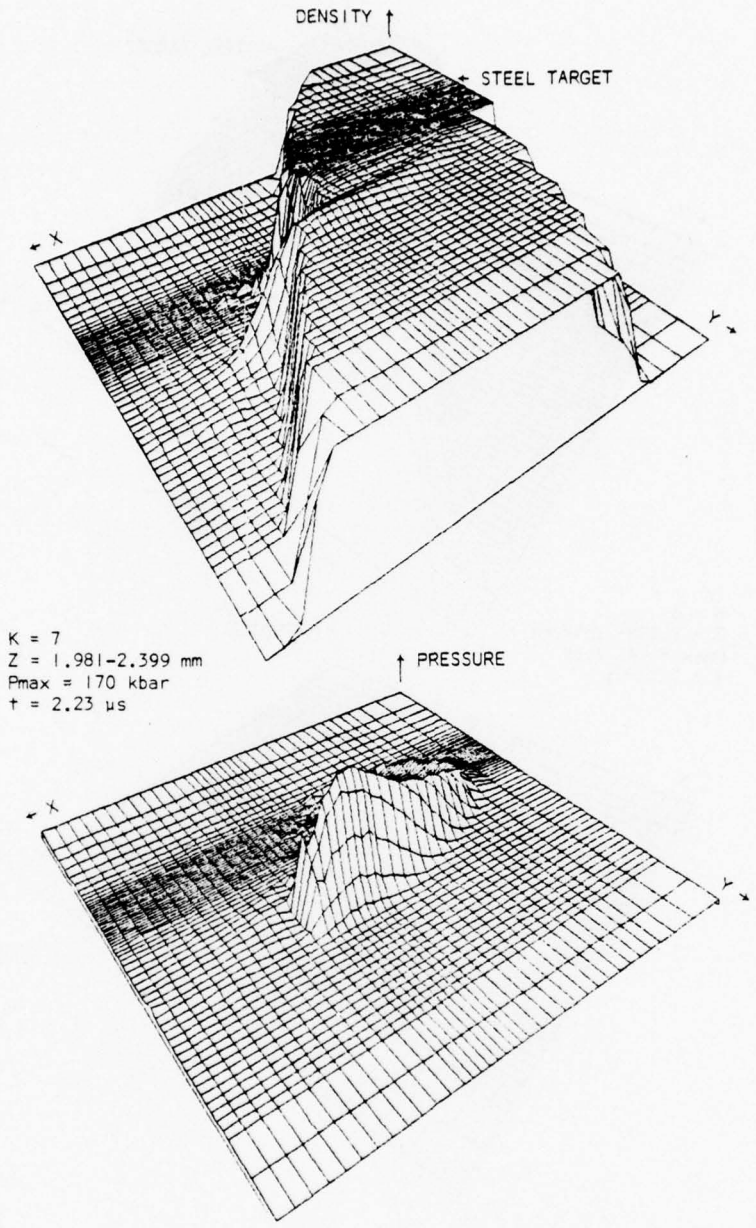

Figure 25. Density and Pressure Fields

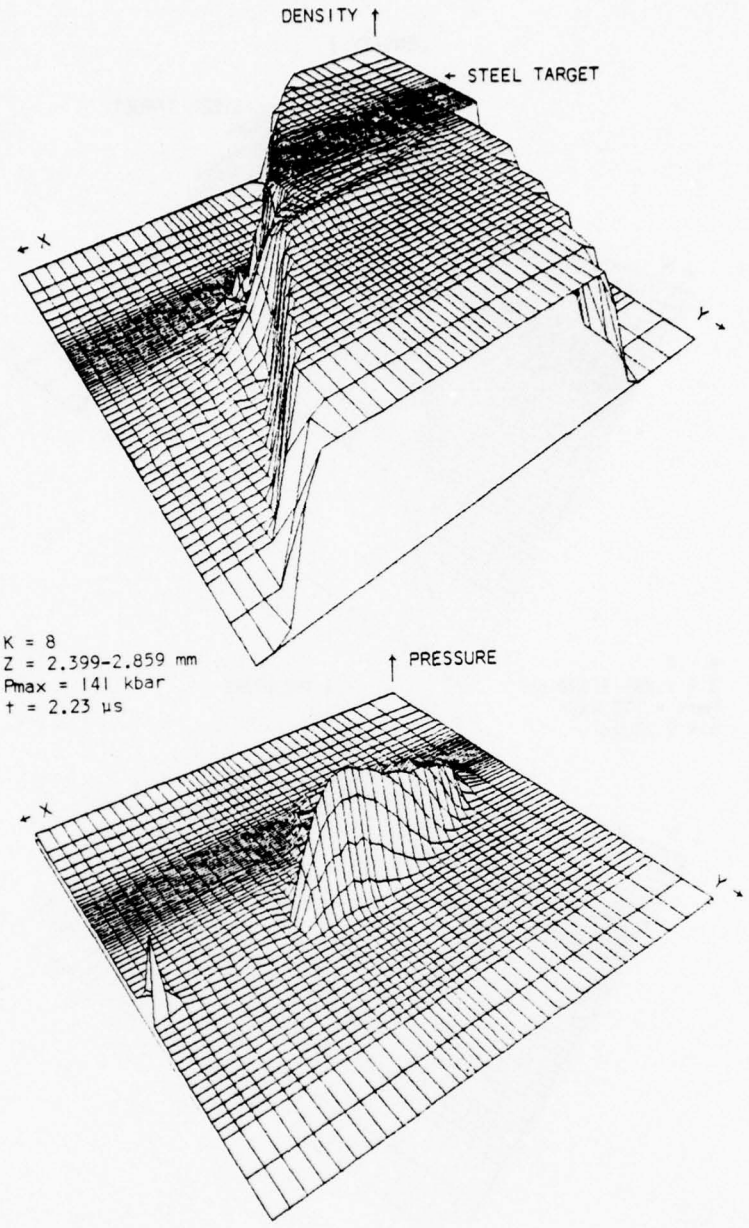

Figure 26. Density and Pressure Fields

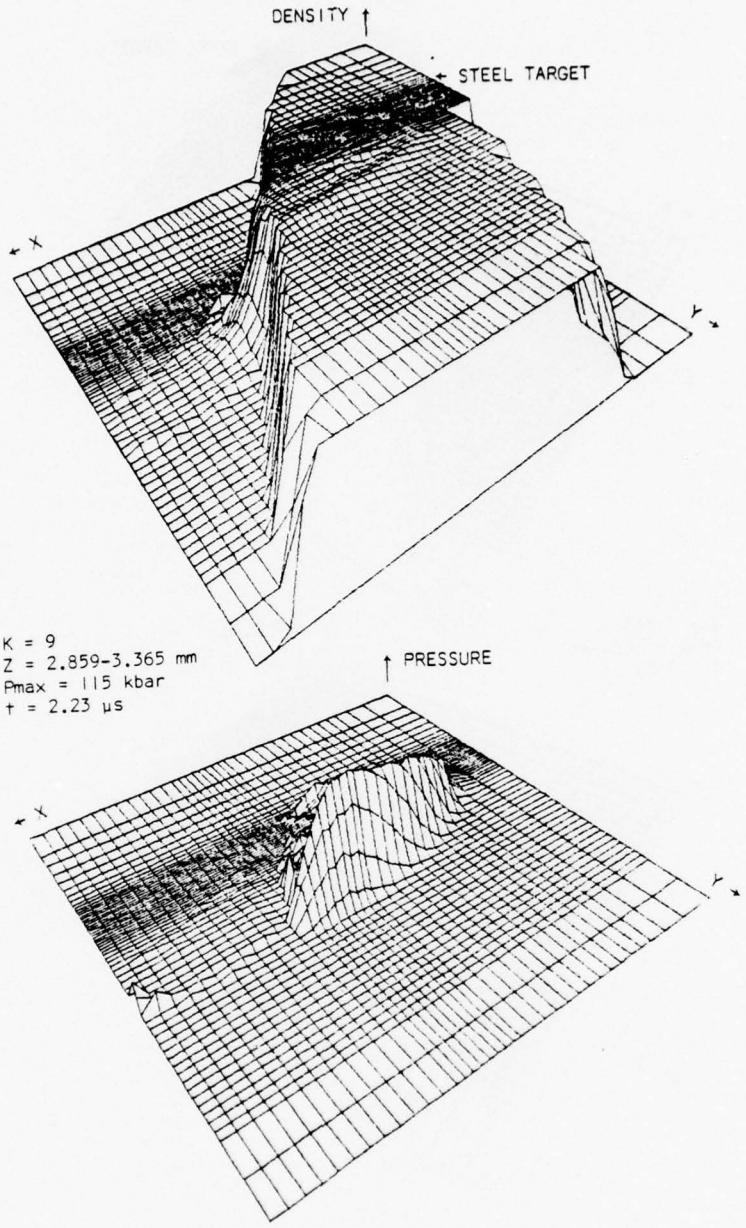

Figure 27. Density and Pressure Fields

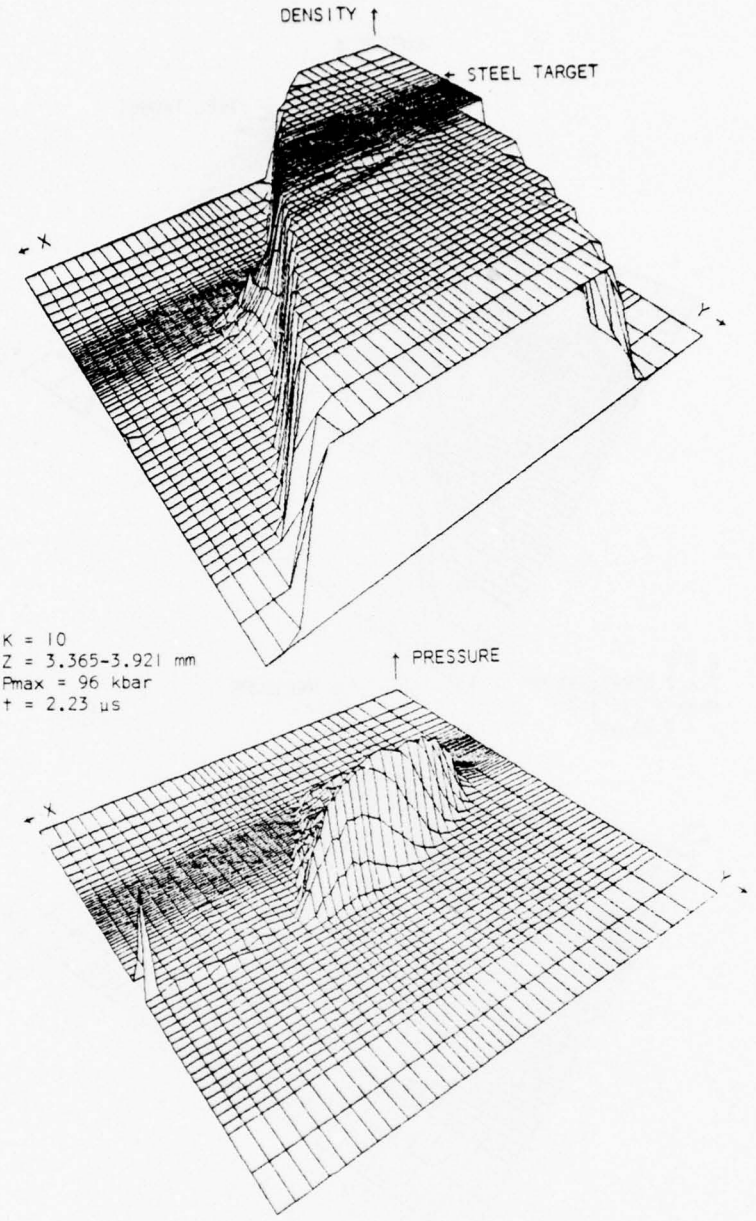

Figure 28. Density and Pressure Fields

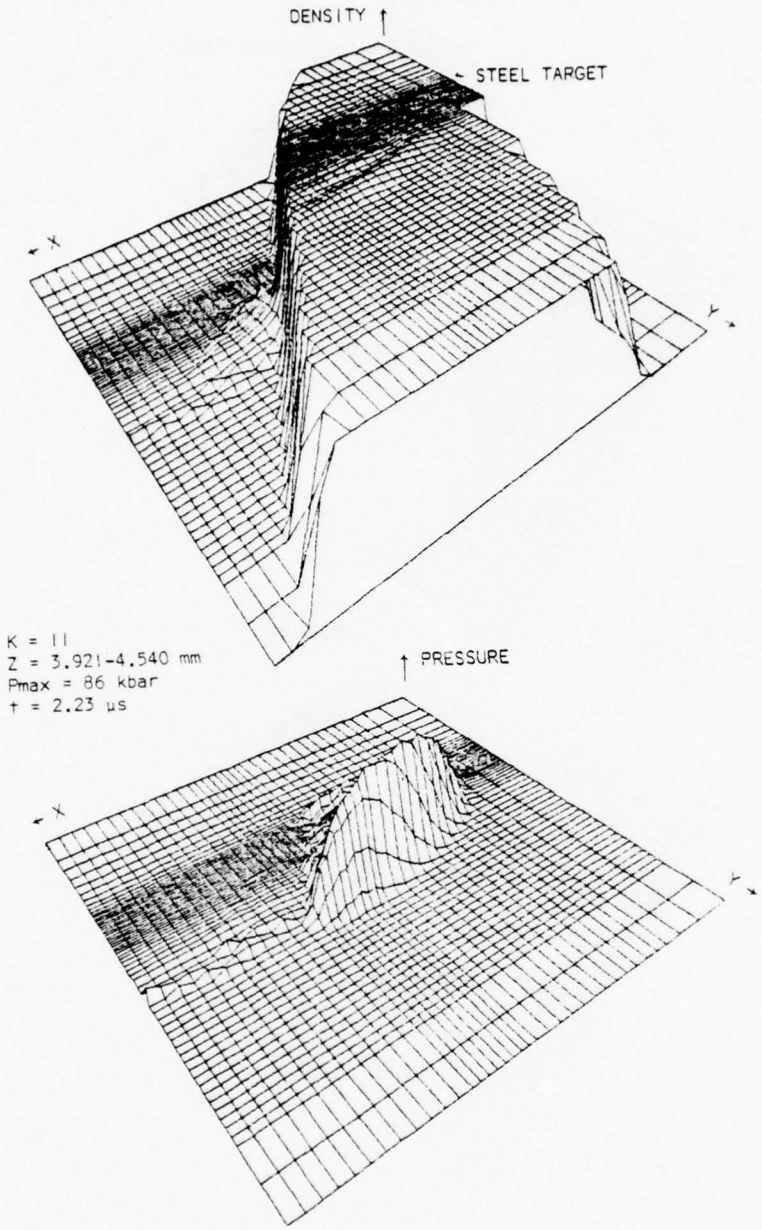

Figure 29. Density and Pressure Fields

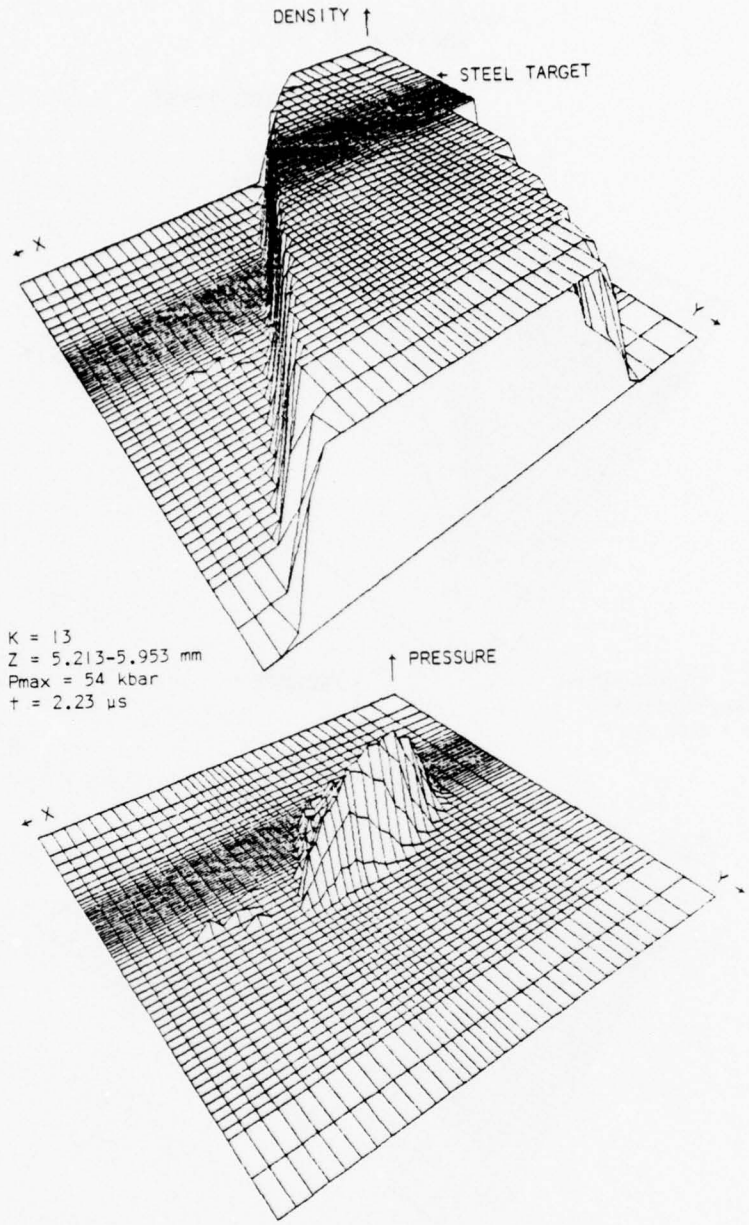

Figure 30. Density and Pressure Fields

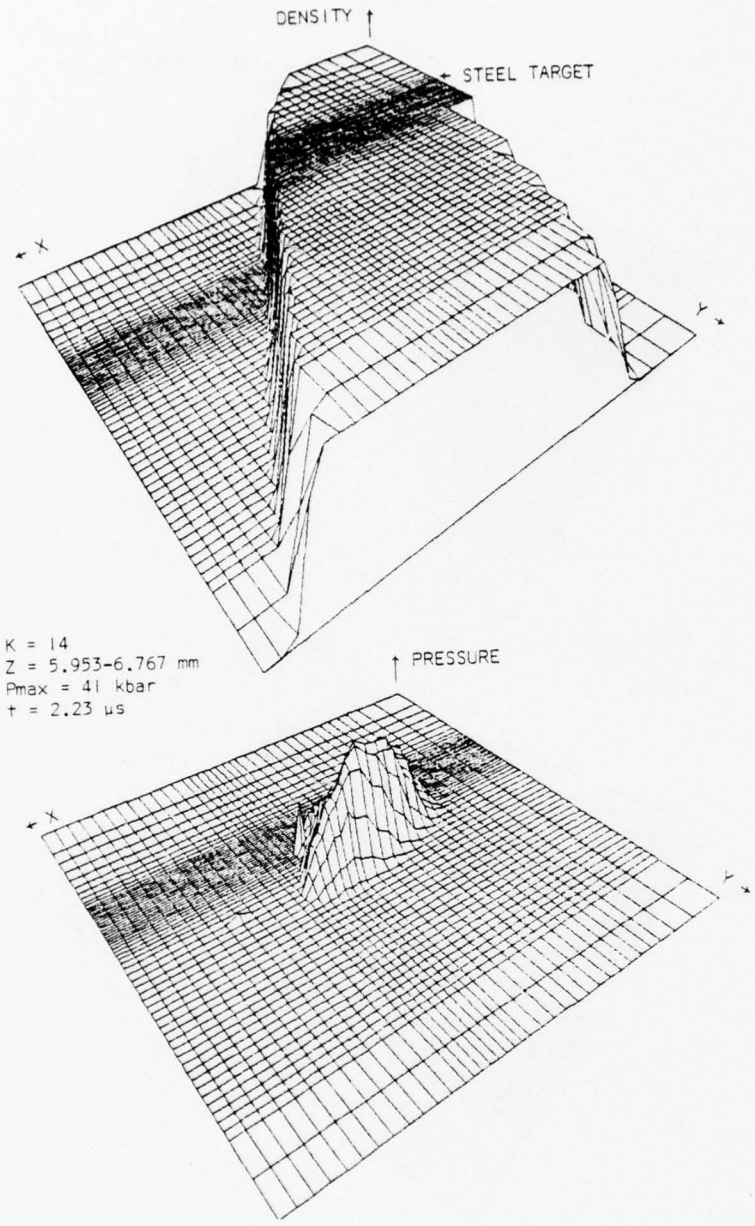

Figure 31. Density and Pressure Fields

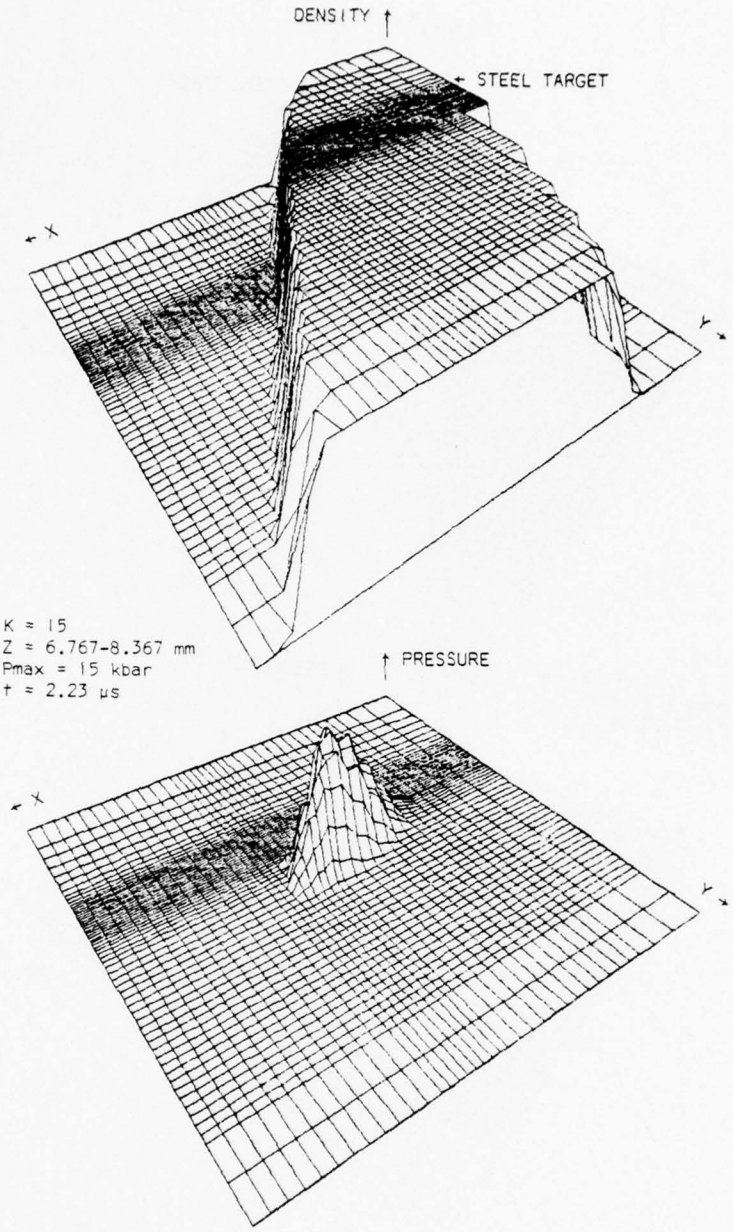

Figure 32. Density and Pressure Fields

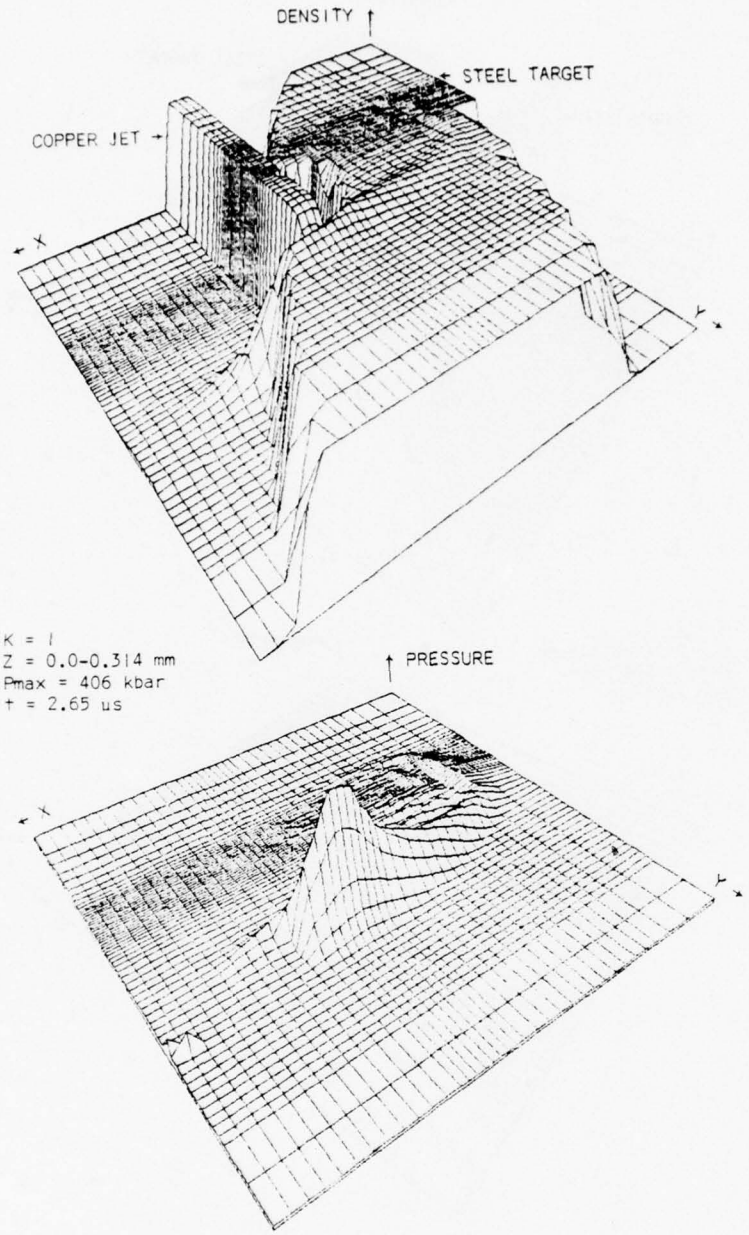

Figure 33. Density and Pressure Fields

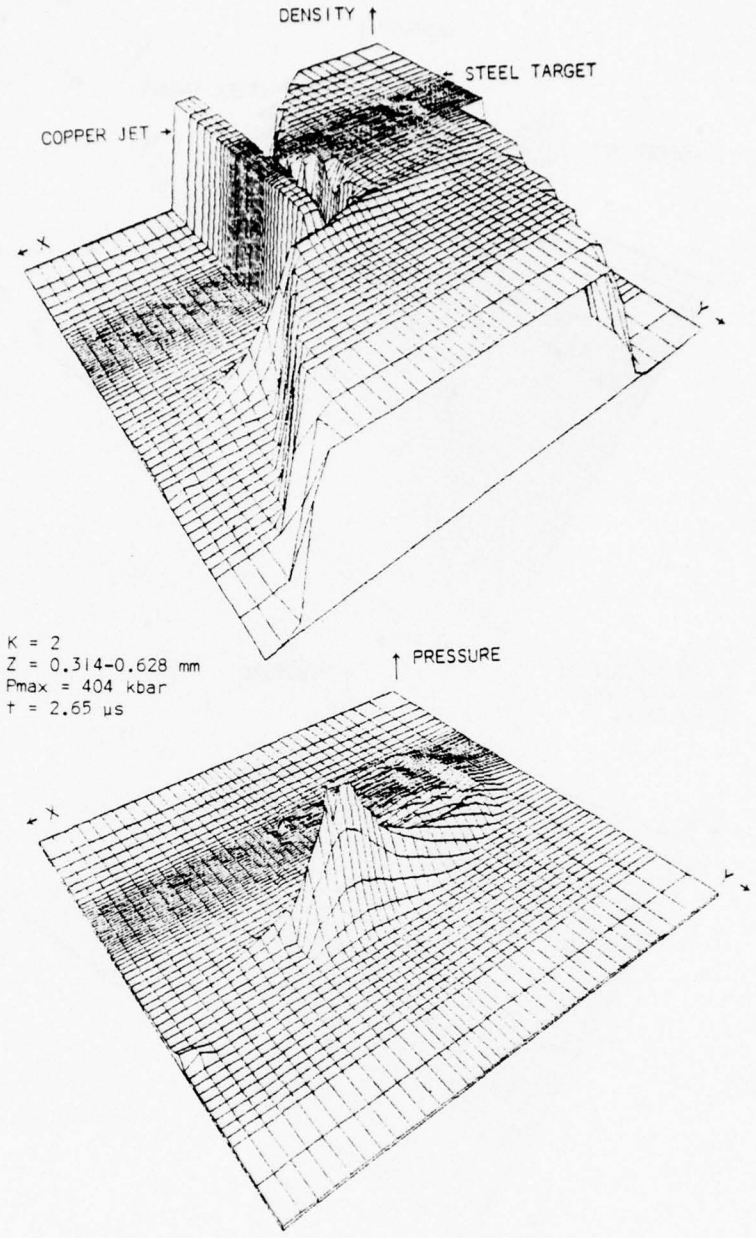

Figure 34. Density and Pressure Fields

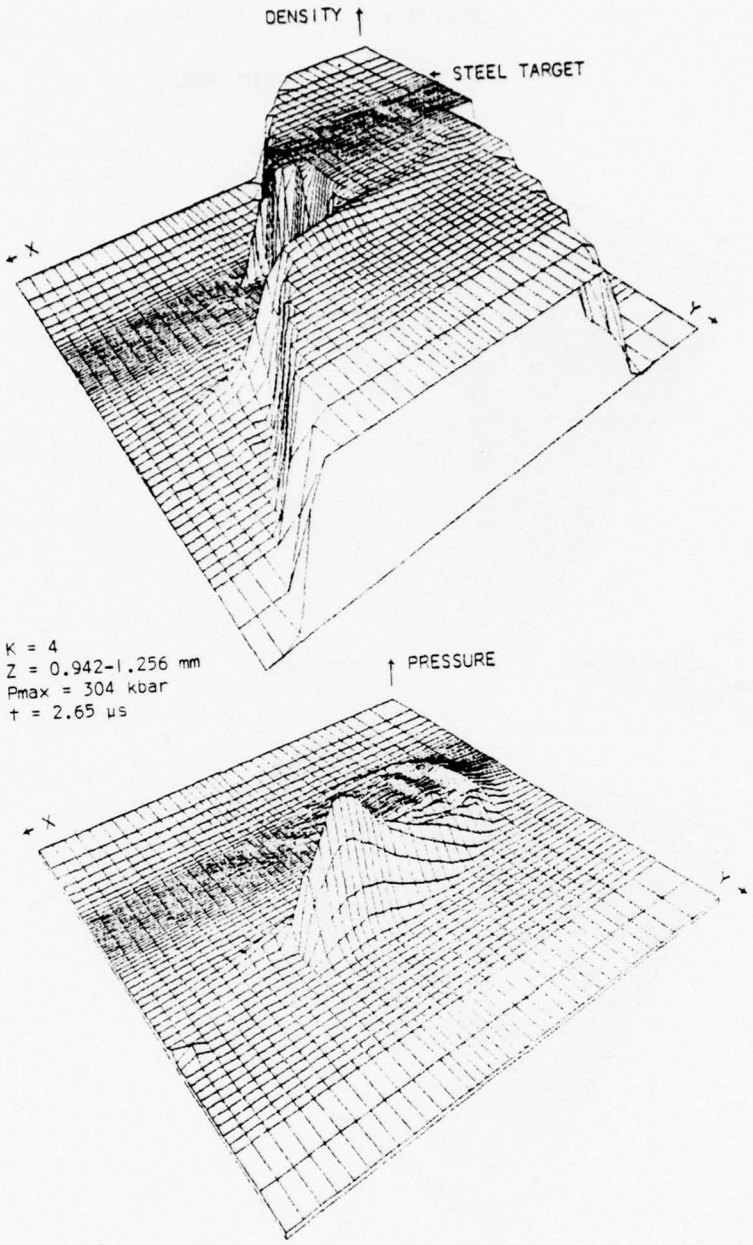

Figure 35. Density and Pressure Fields

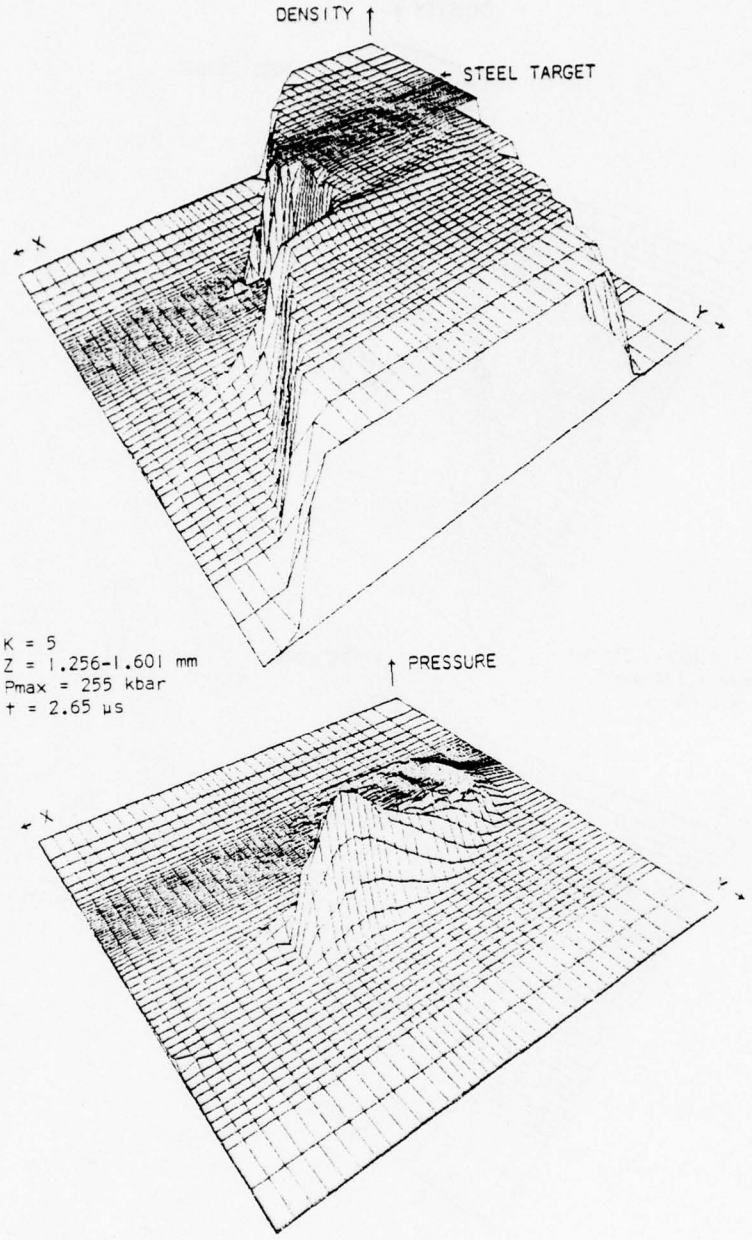

Figure 36. Density and Pressure Fields

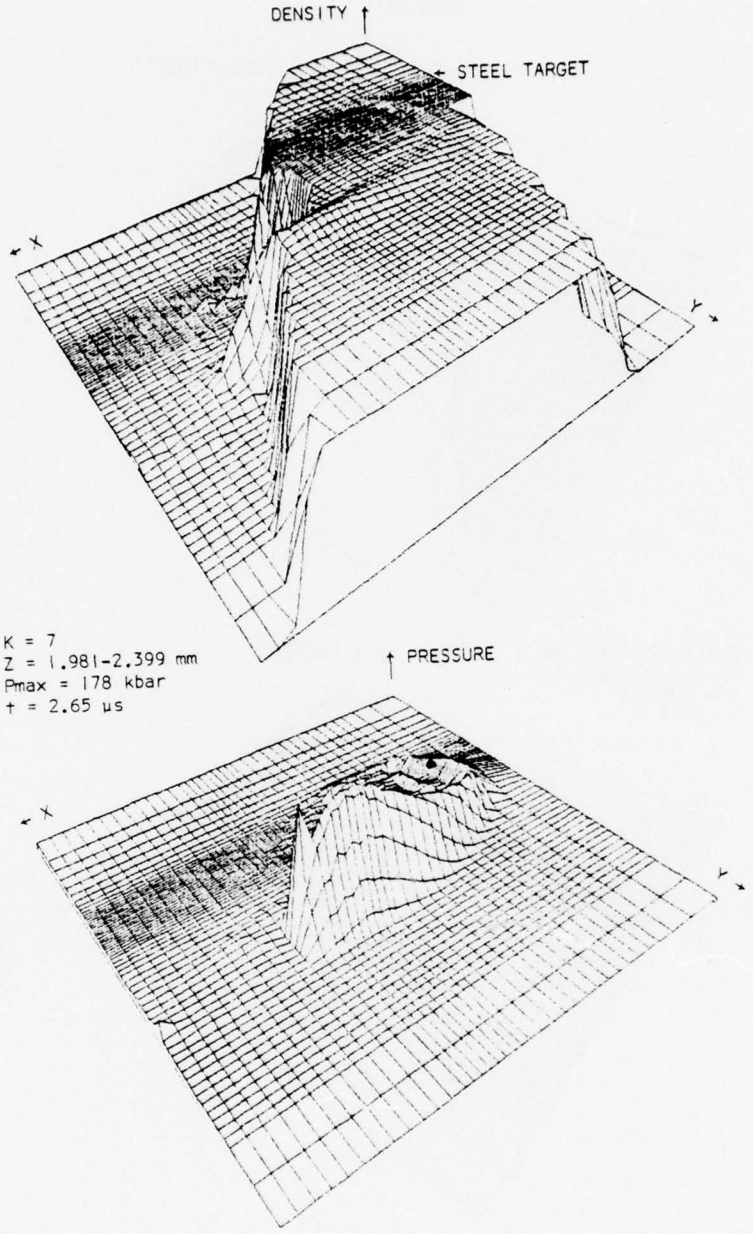

Figure 37. Density and Pressure Fields

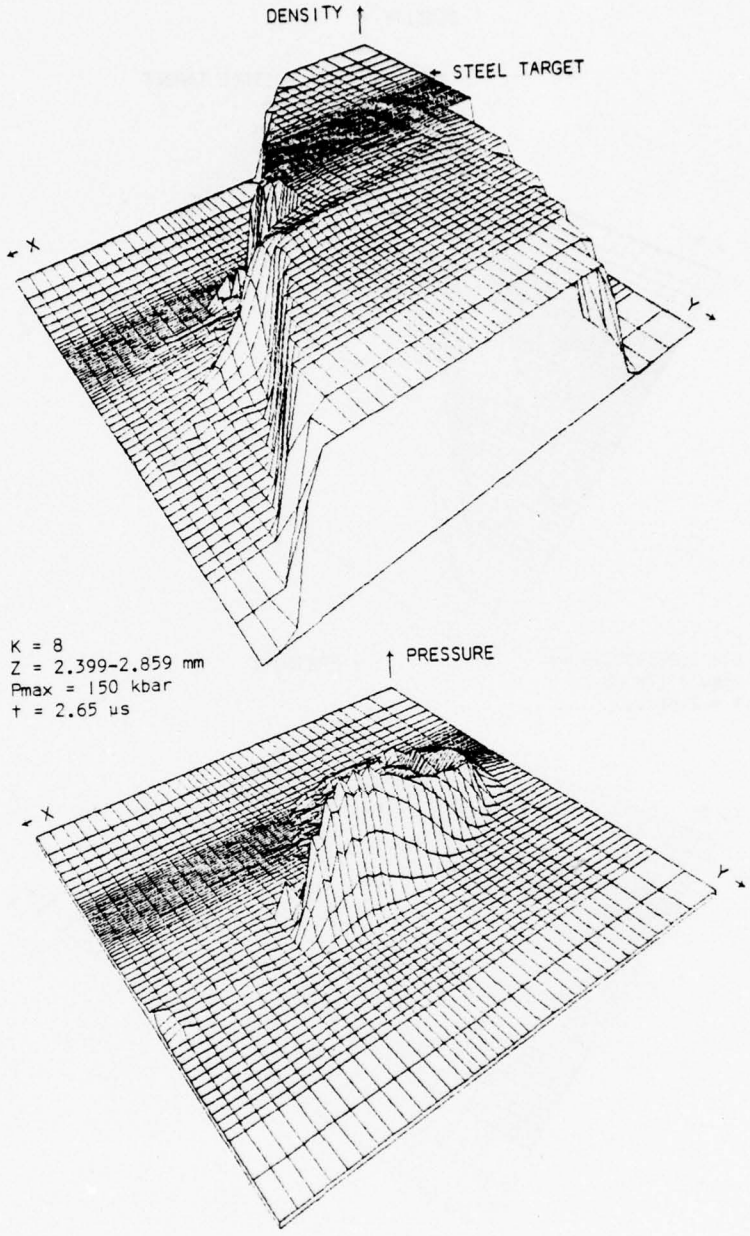

Figure 38. Density and Pressure Fields

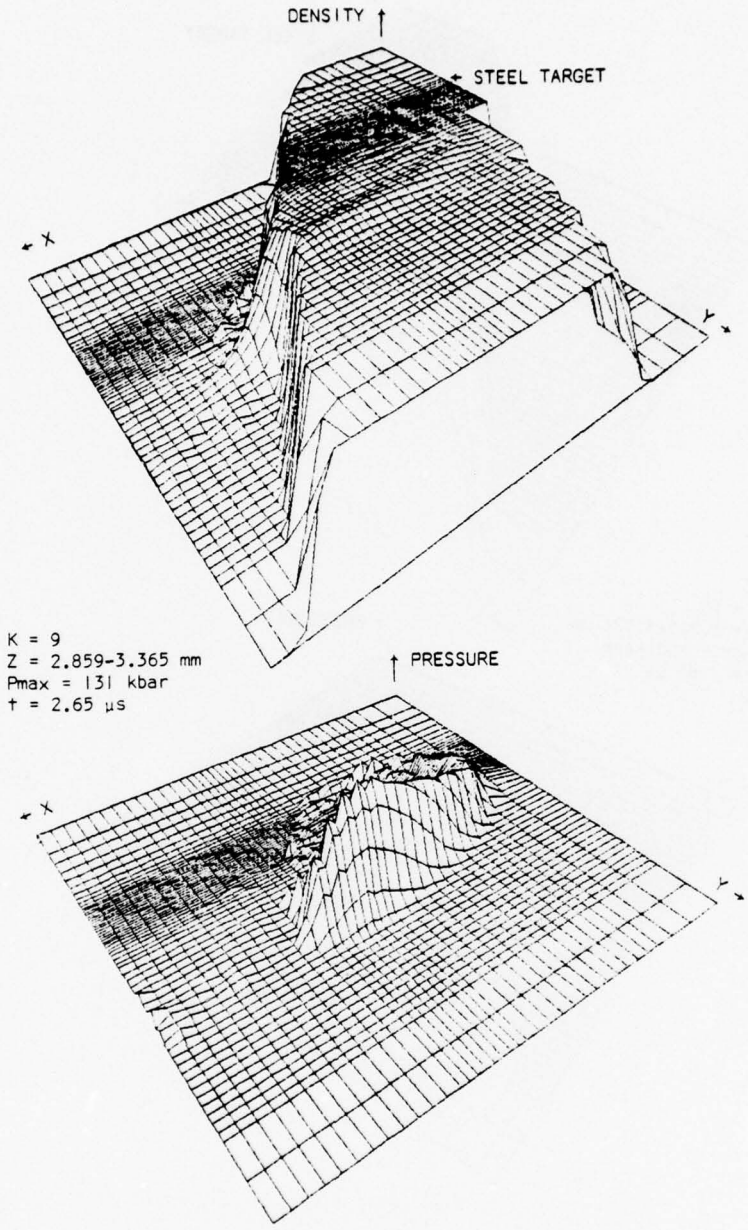

Figure 39. Density and Pressure Fields

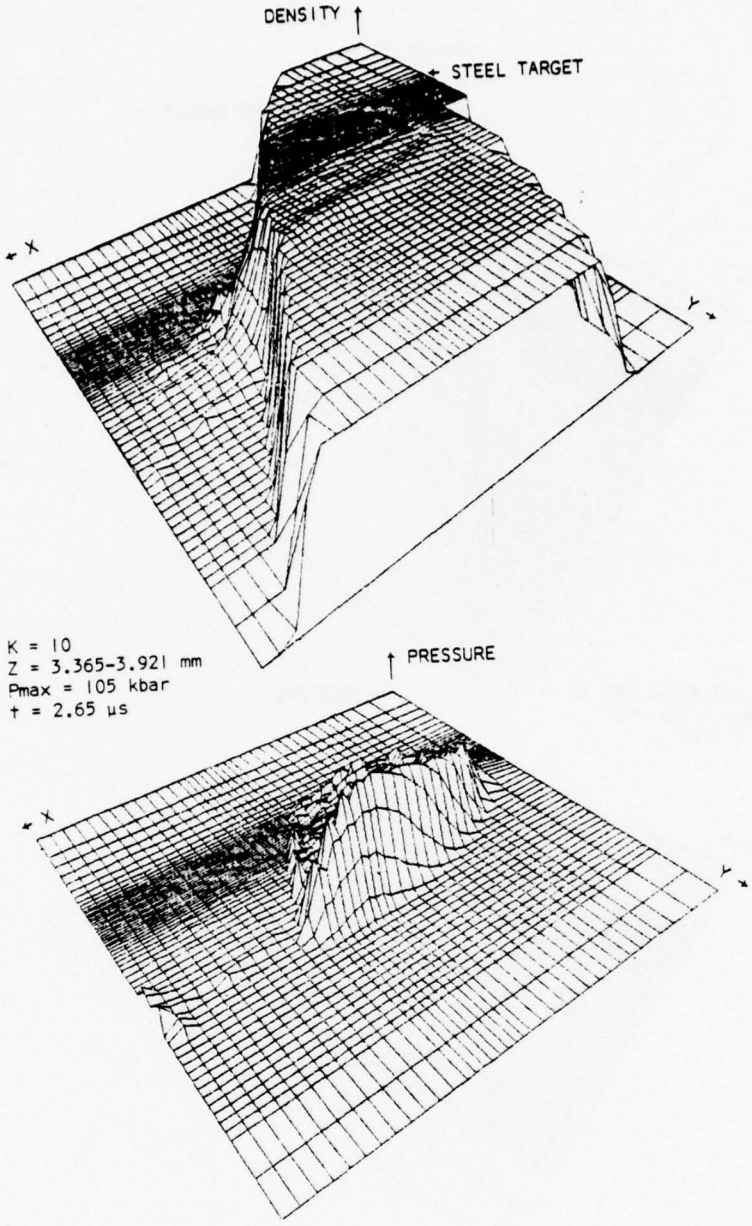

Figure 40. Density and Pressure Fields

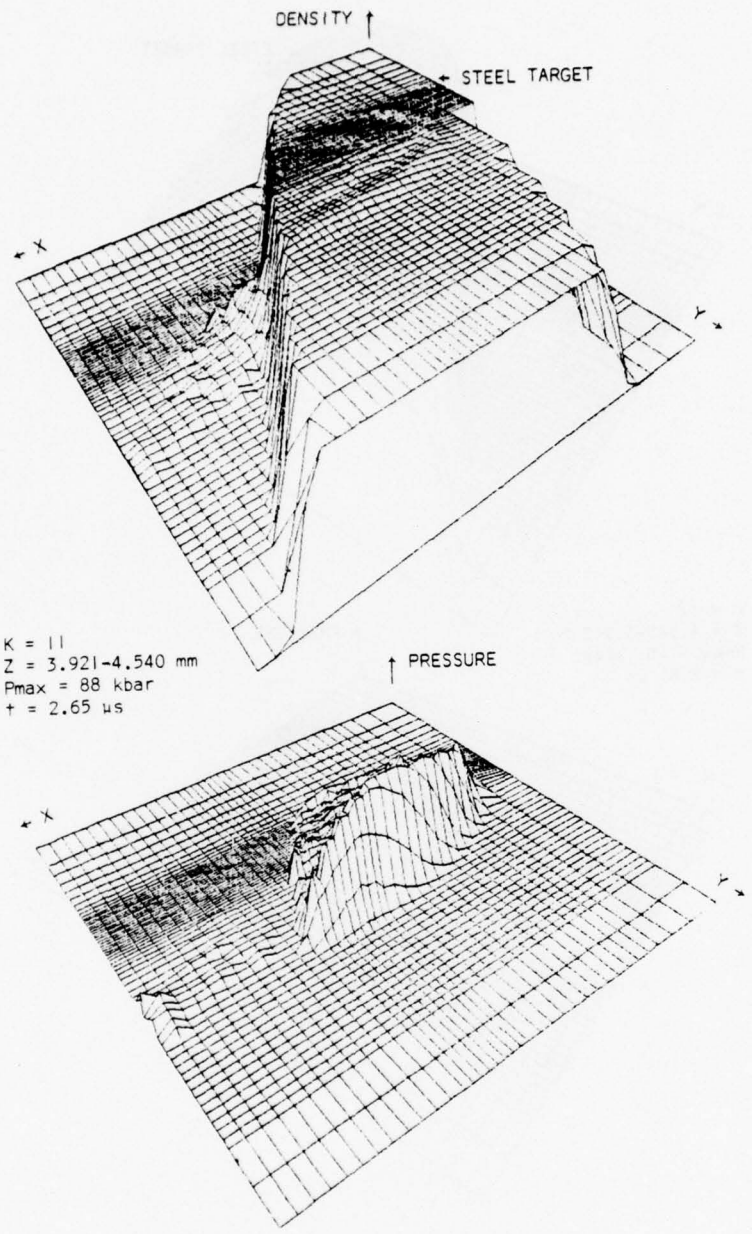

Figure 41. Density and Pressure Fields

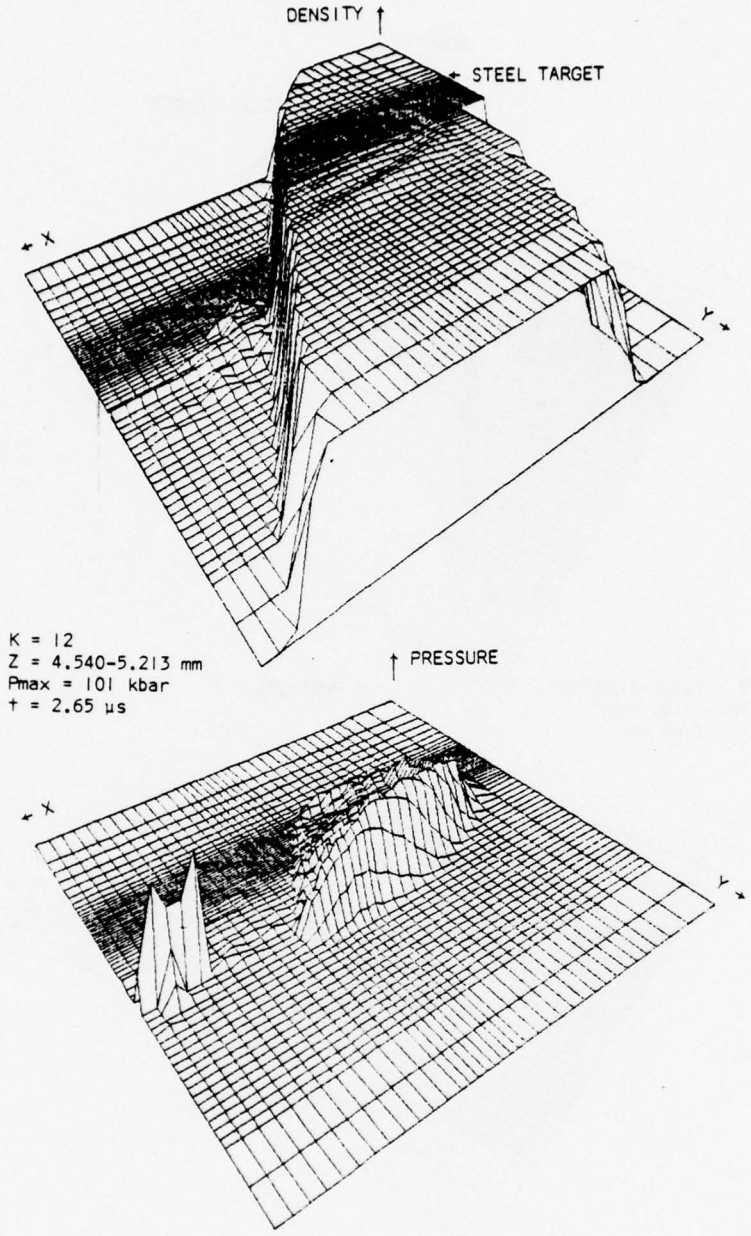

Figure 42. Density and Pressure Fields

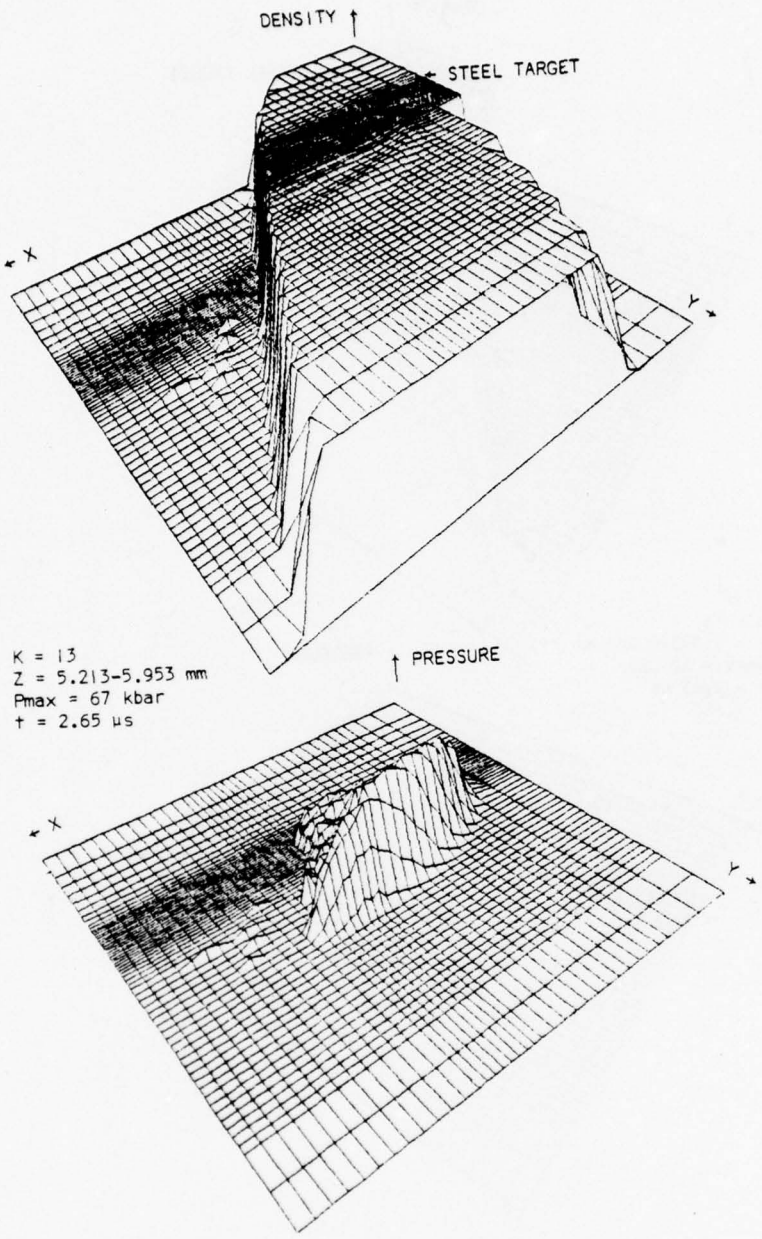

Figure 43. Density and Pressure Fields

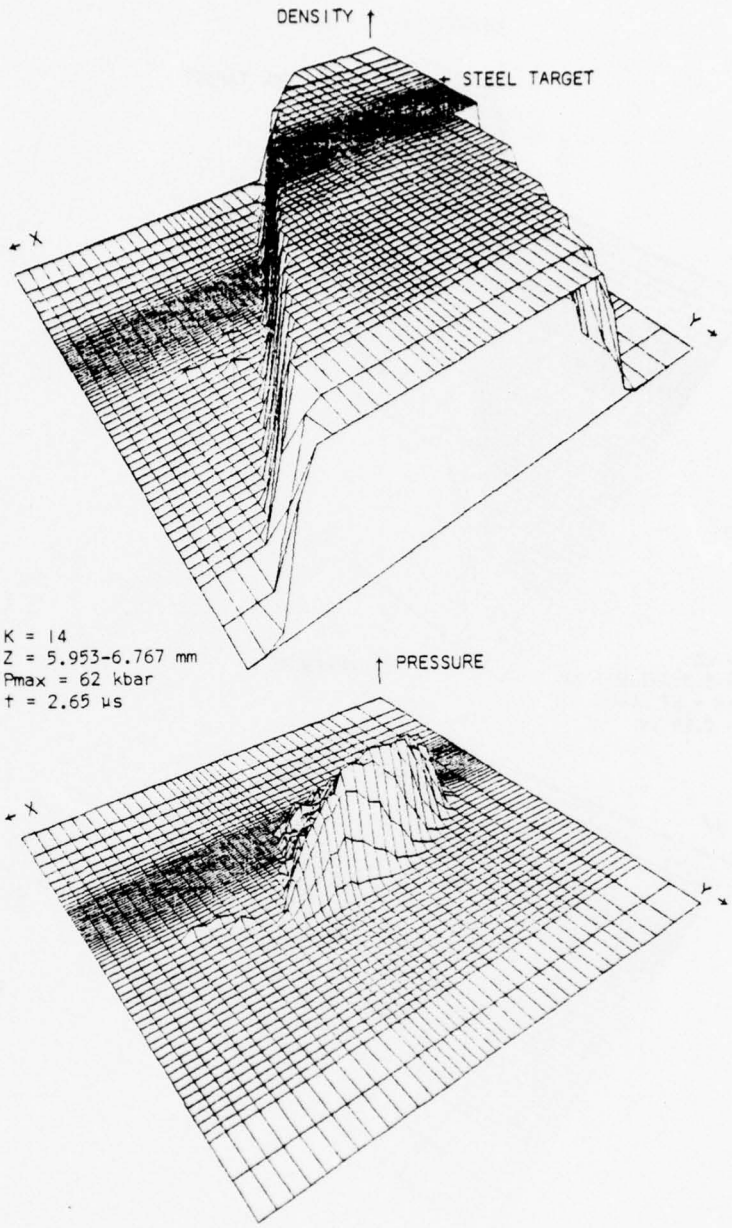

Figure 44. Density and Pressure Fields

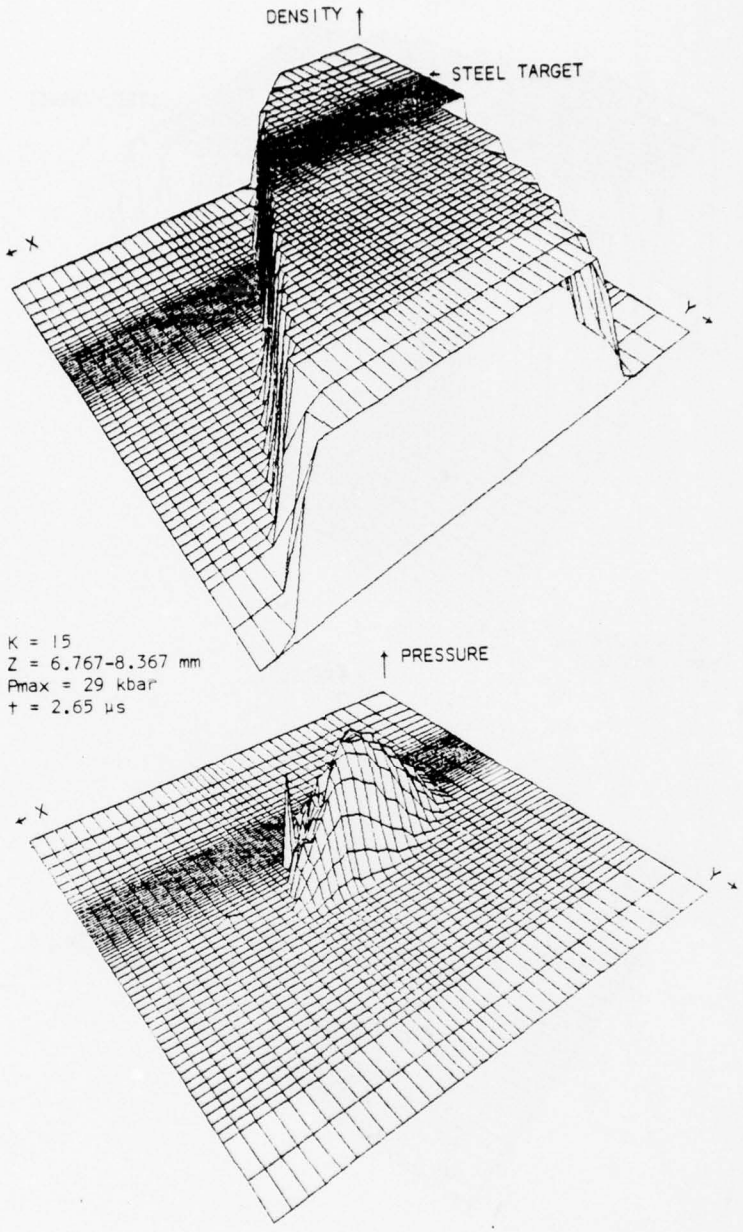

Figure 45. Density and Pressure Fields

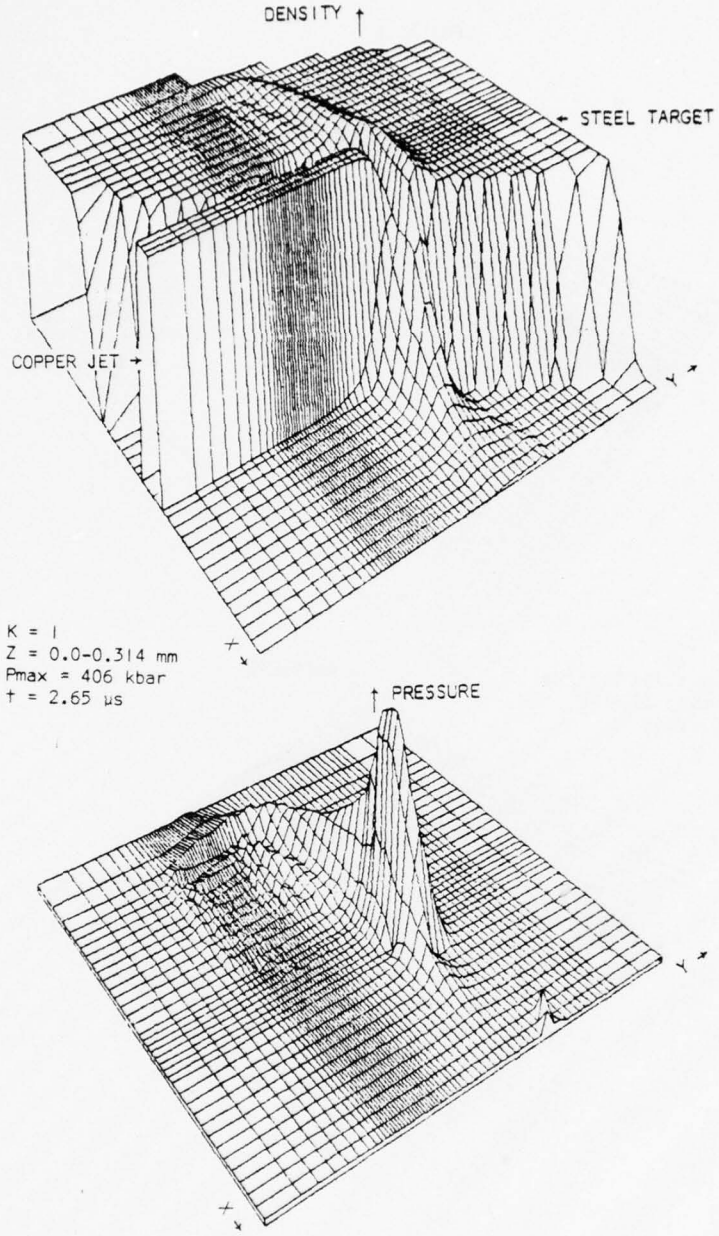

Figure 46. Density and Pressure Fields

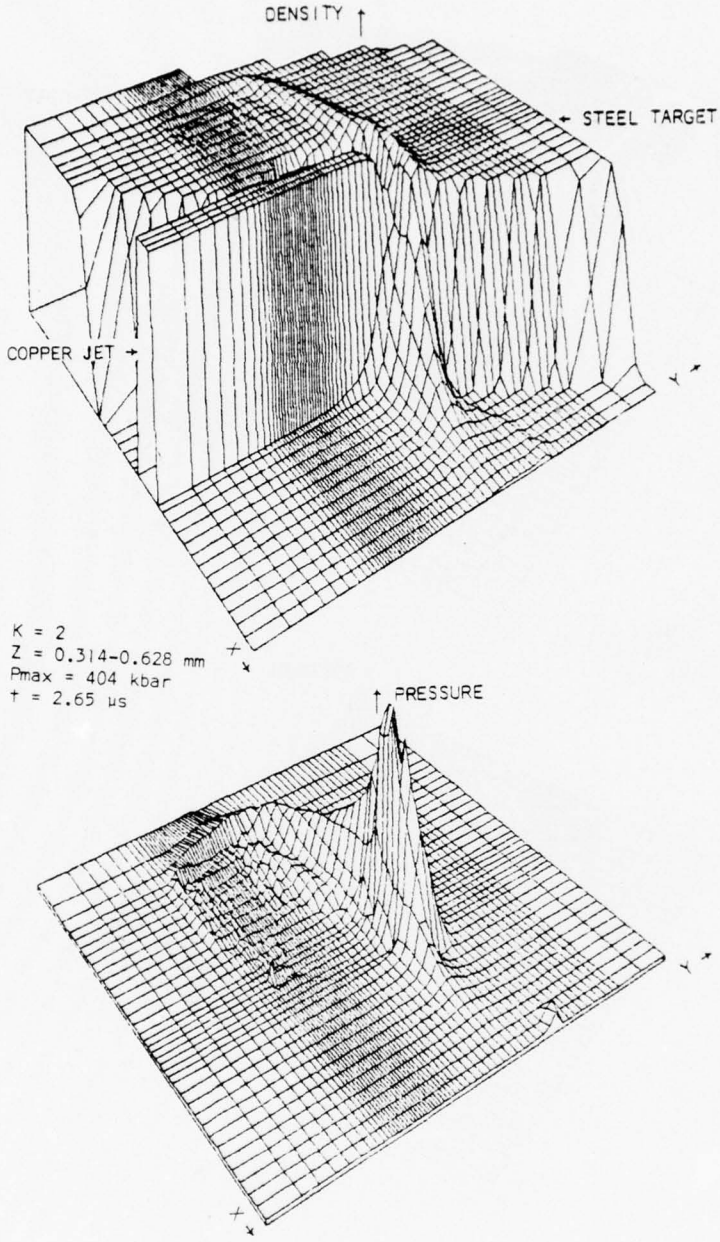

Figure 47. Density and Pressure Fields

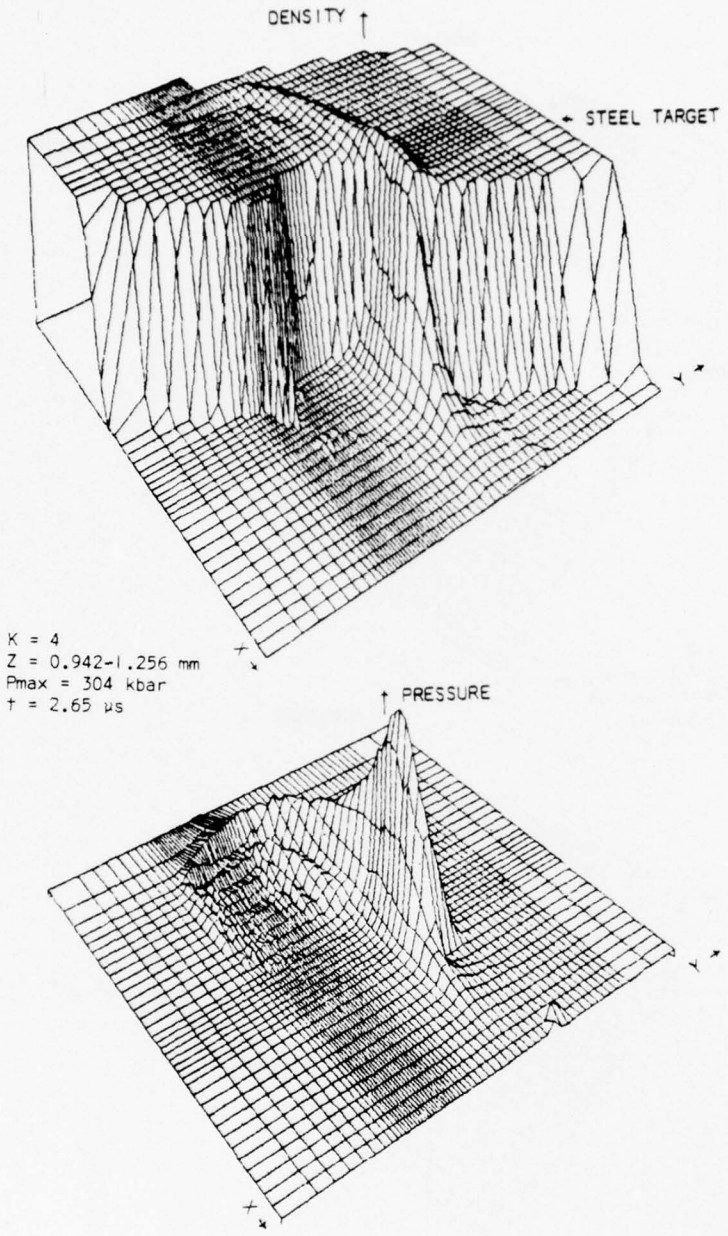

Figure 48. Density and Pressure Fields

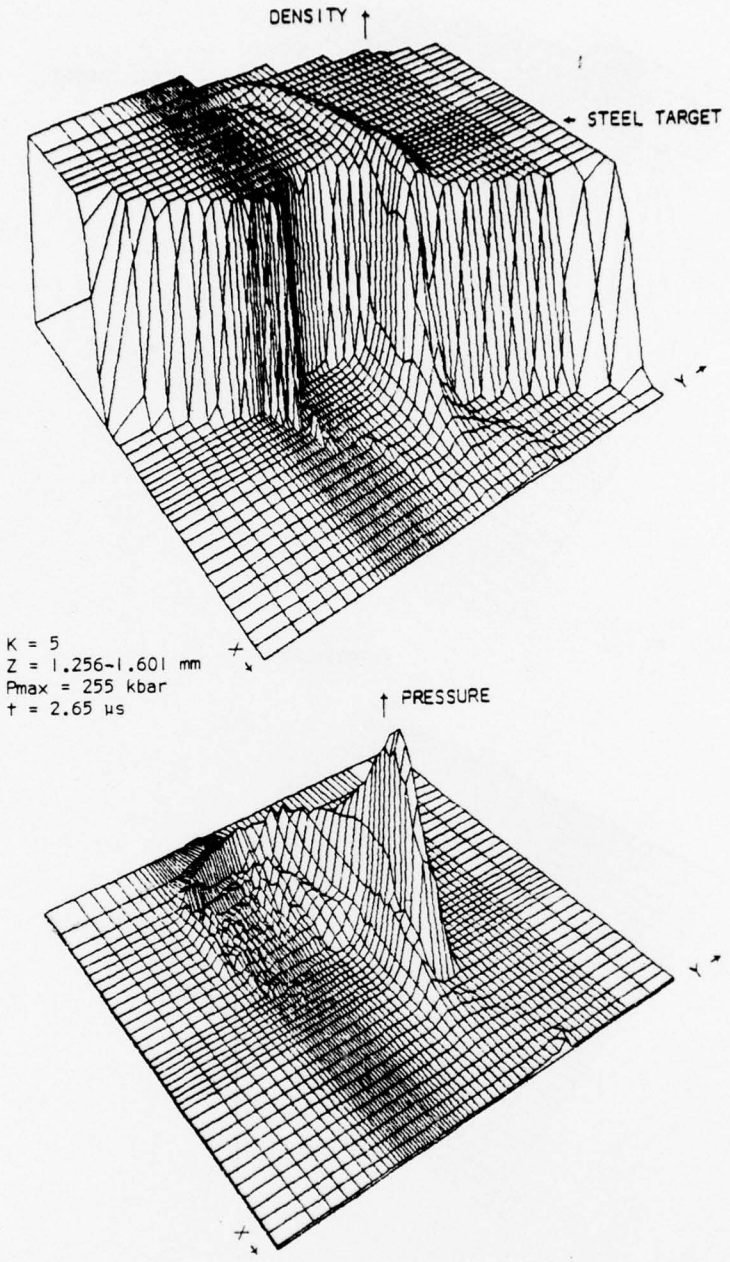

Figure 49. Density and Pressure Fields

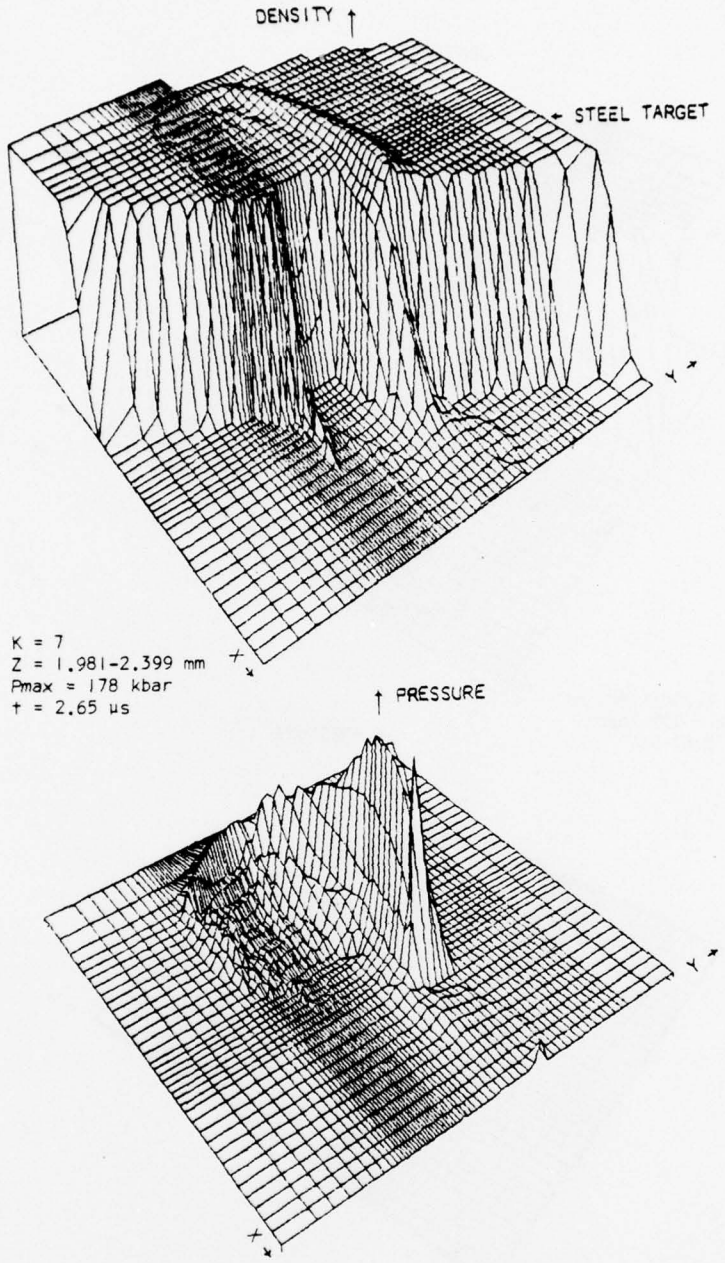

Figure 50. Density and Pressure Fields

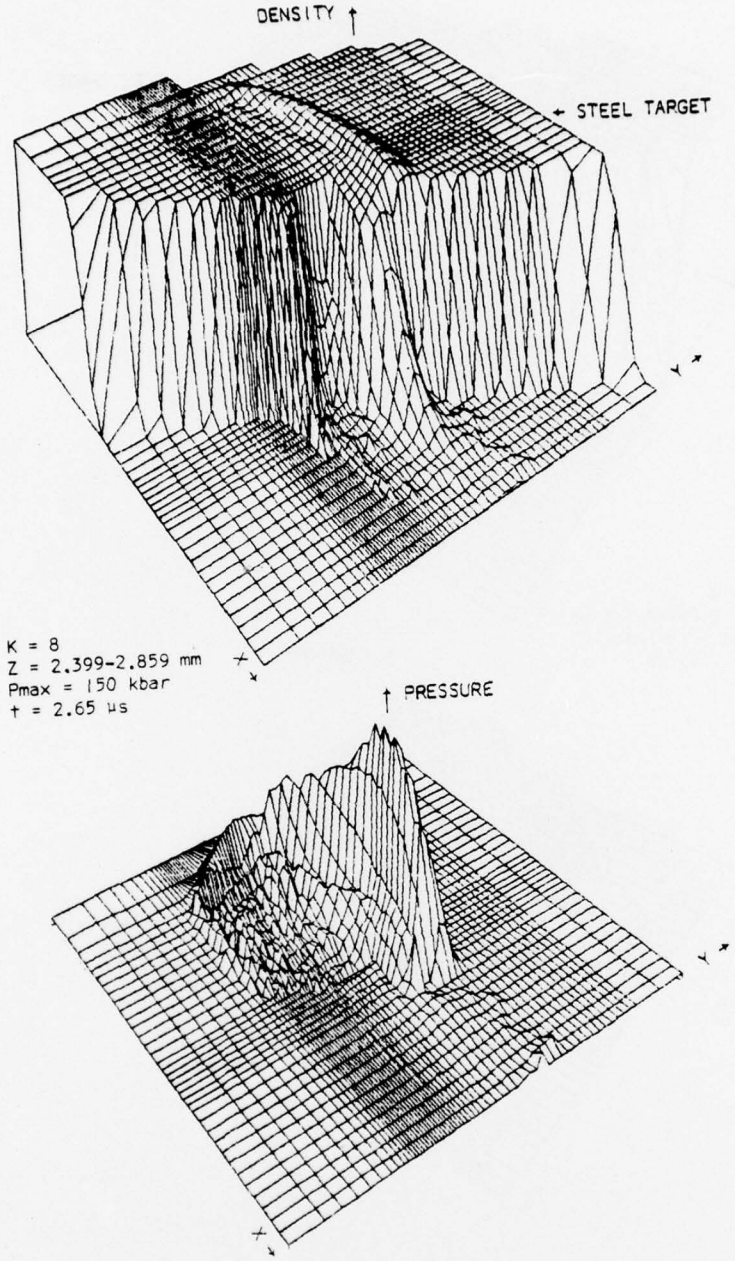

Figure 51. Density and Pressure Fields

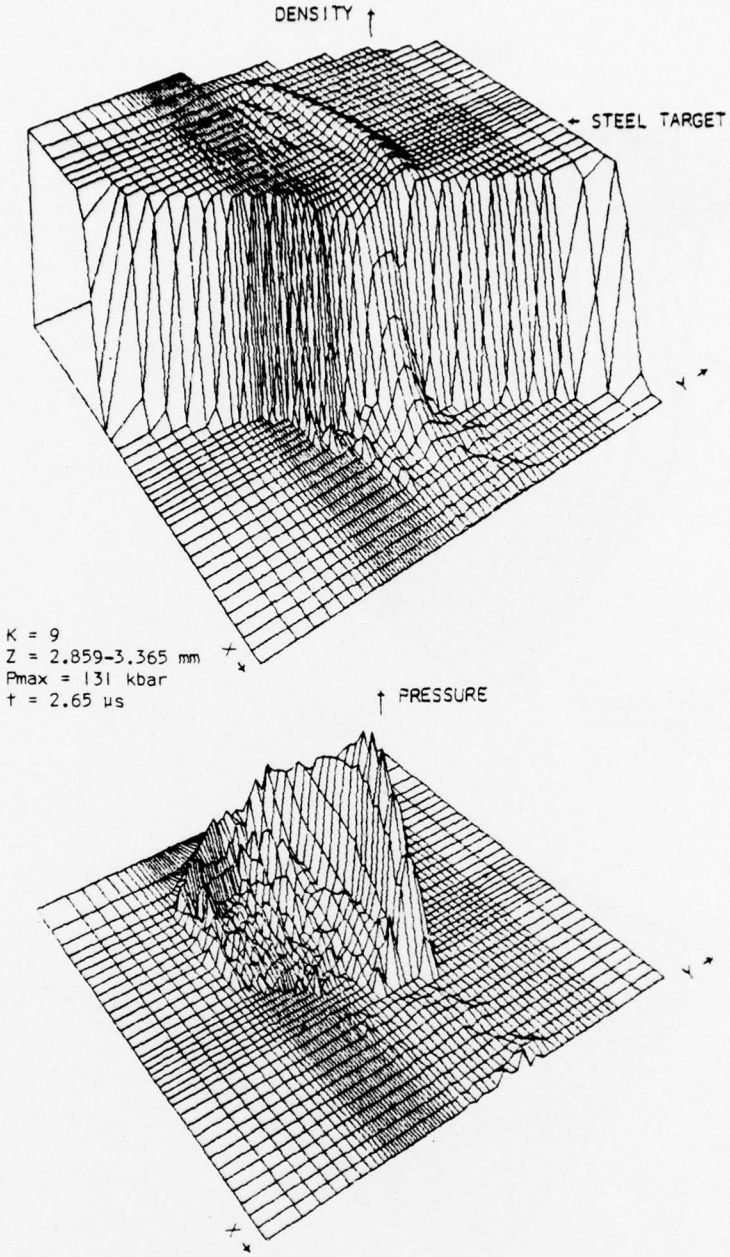

Figure 52. Density and Pressure Fields

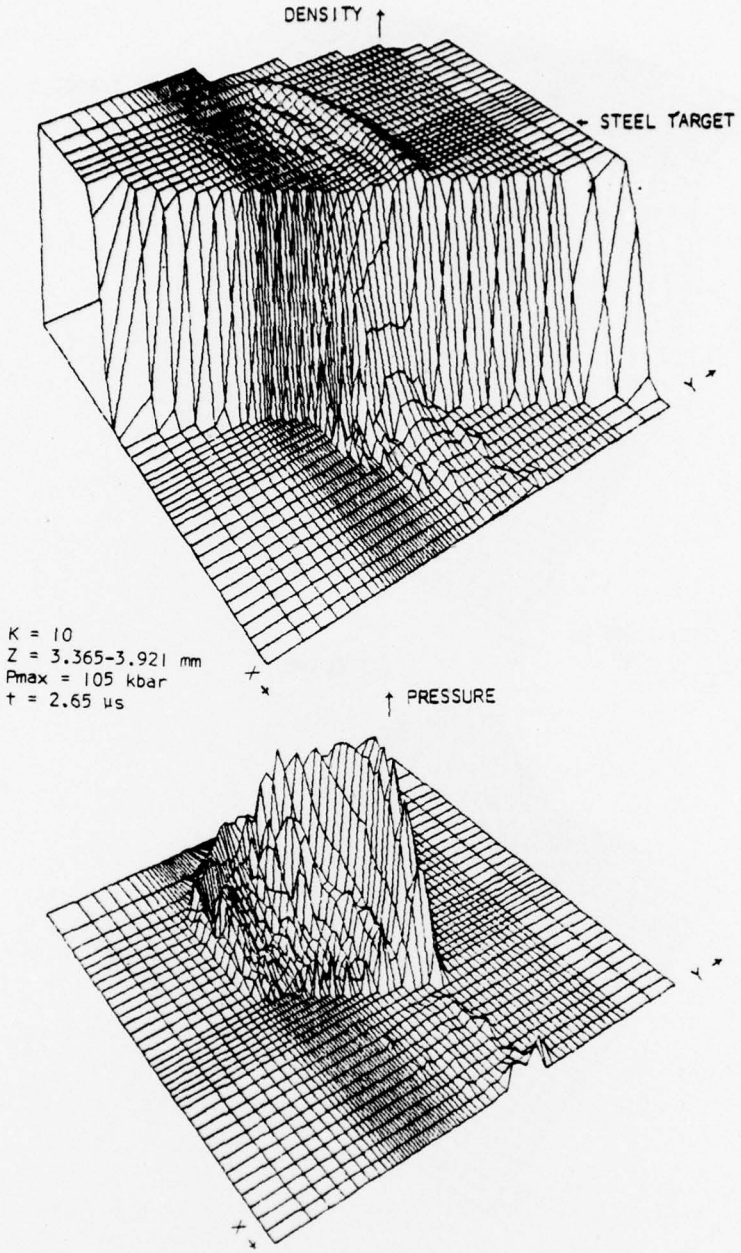

Figure 53. Density and Pressure Fields

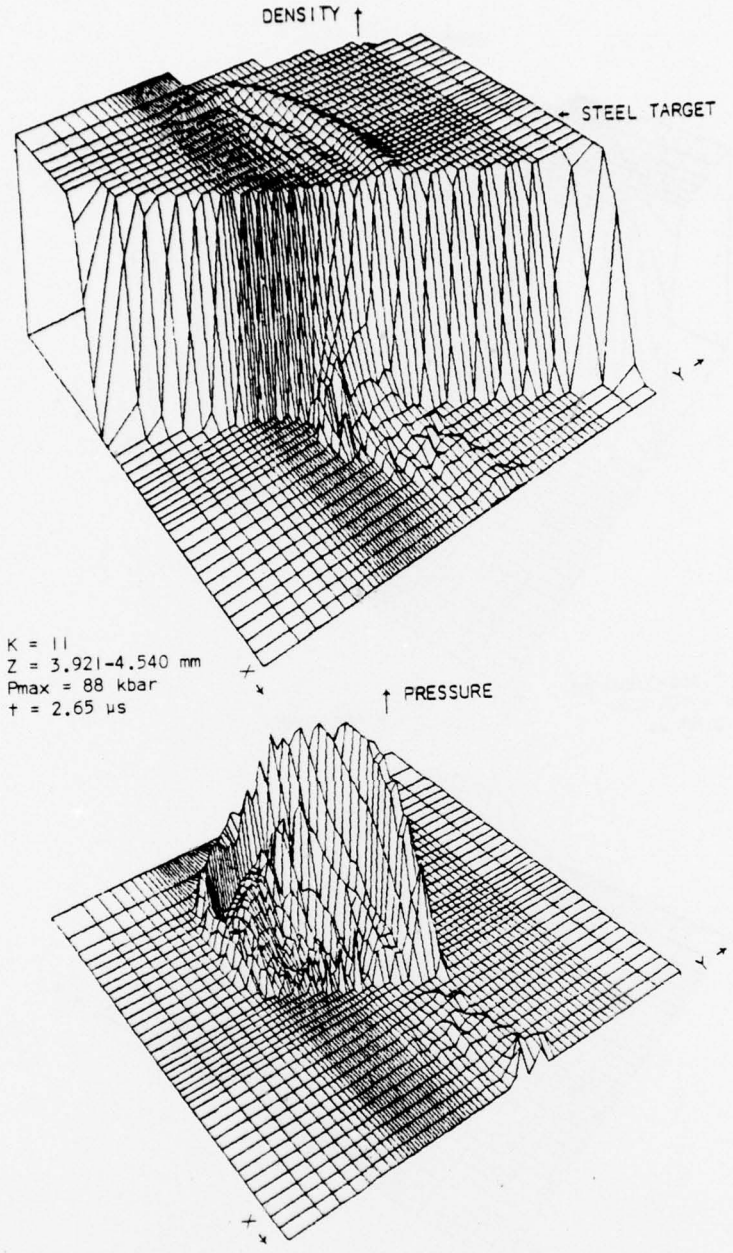

Figure 54. Density and Pressure Fields

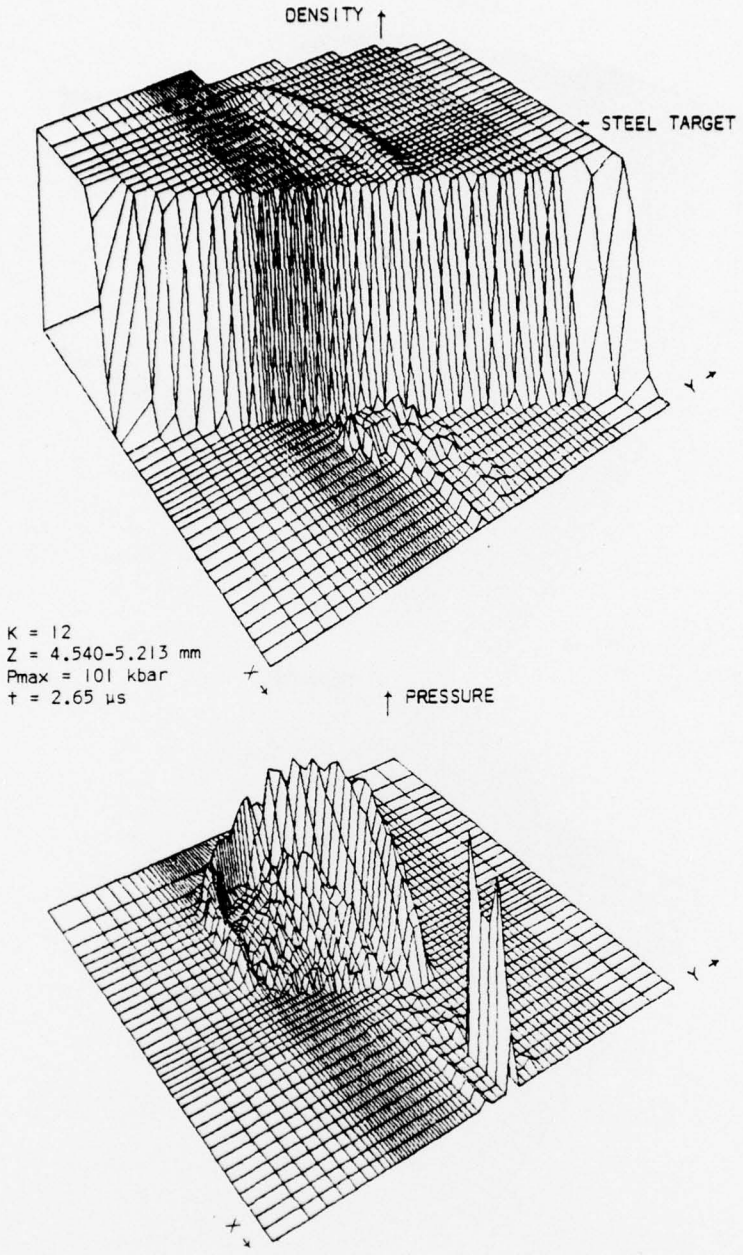

Figure 55. Density and Pressure Fields

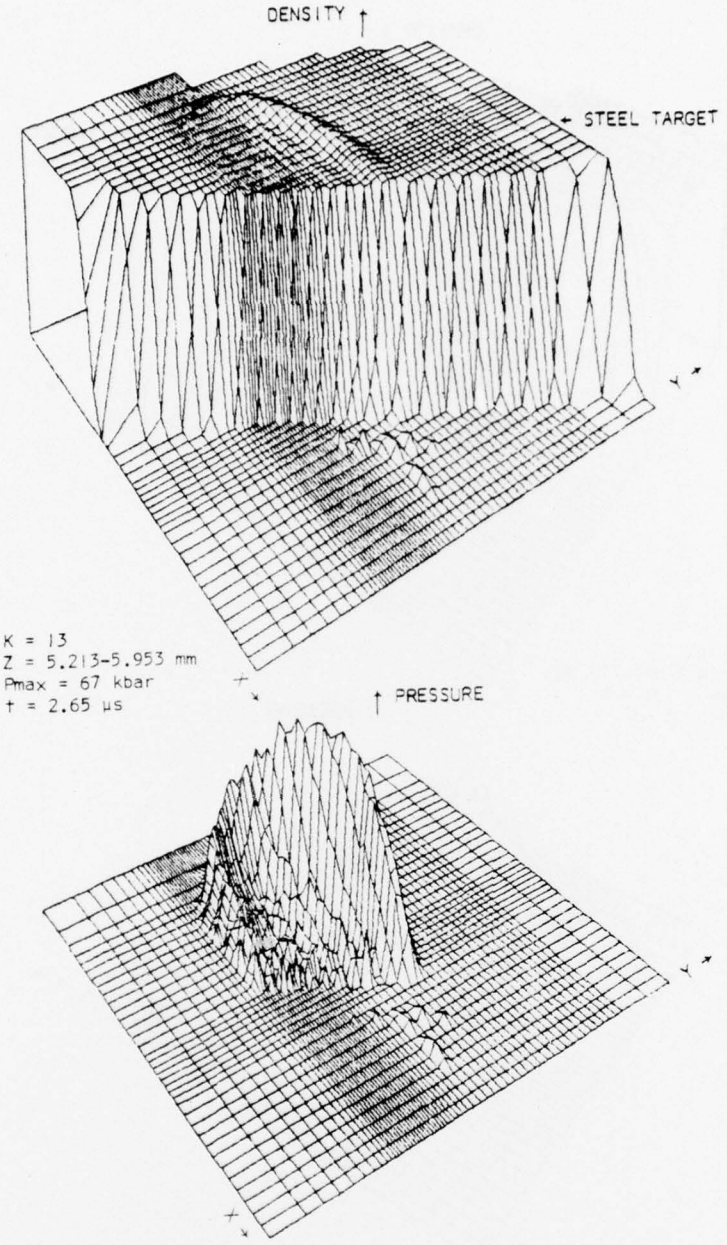

Figure 56. Density and Pressure Fields

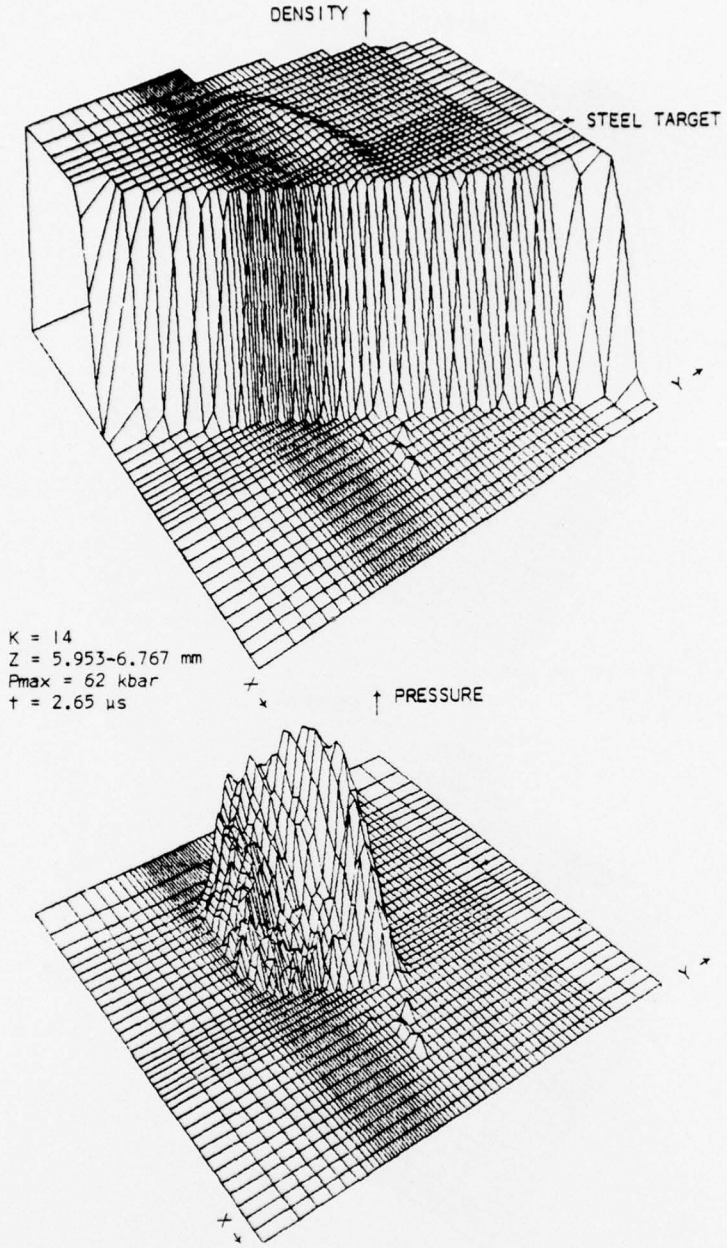

Figure 57. Density and Pressure Fields

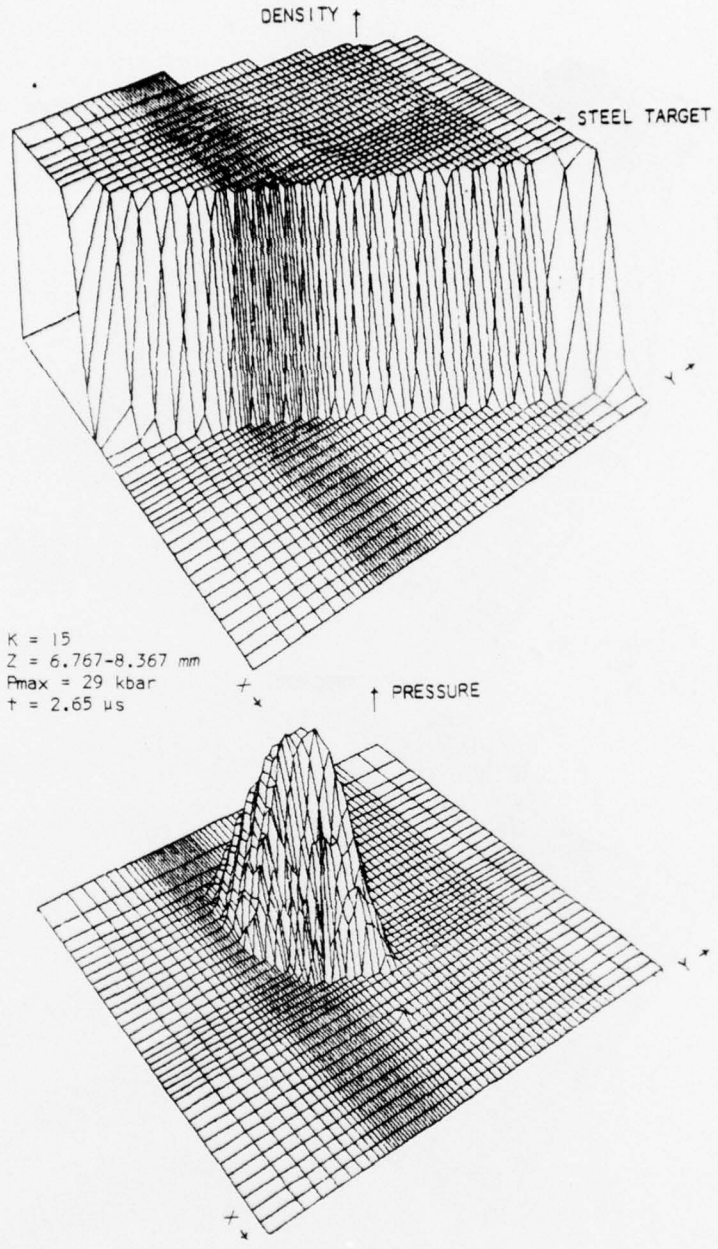

Figure 58. Density and Pressure Fields

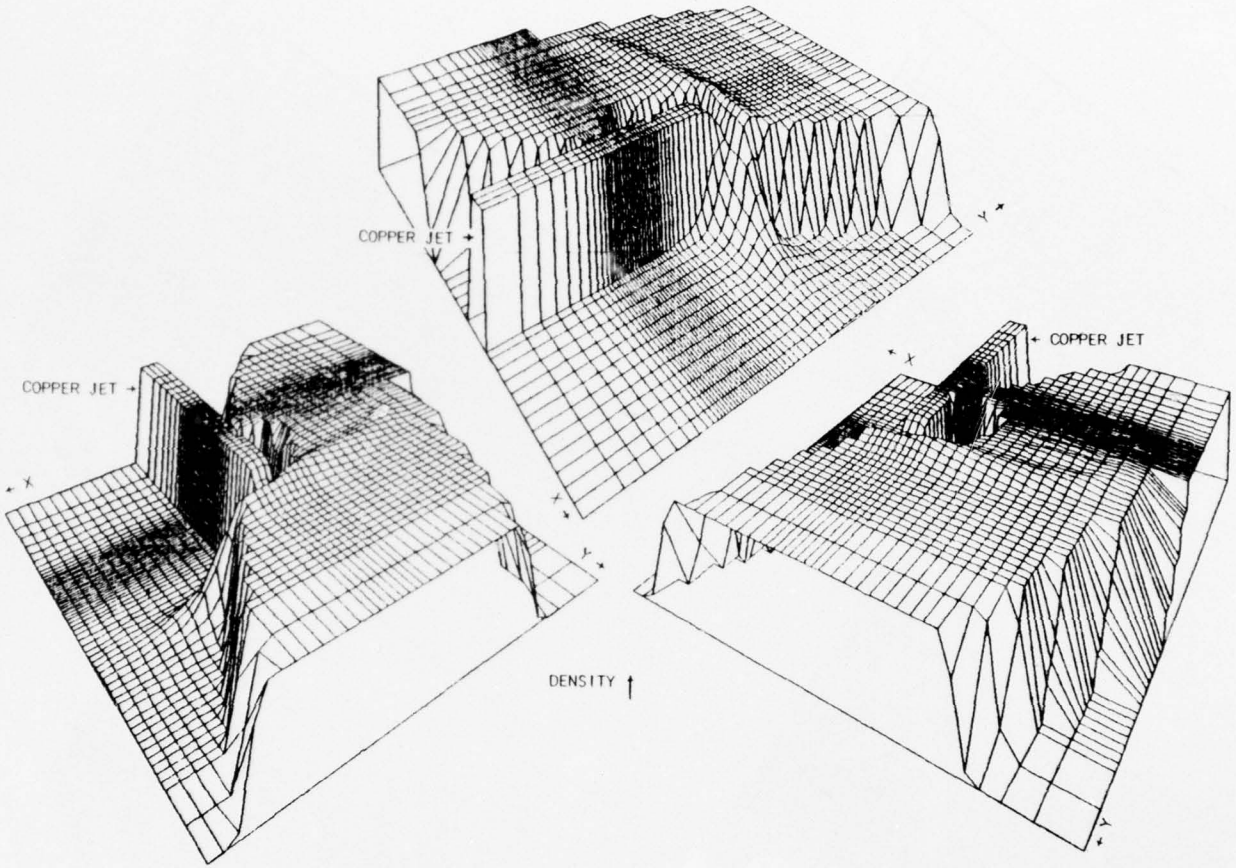

Figure 59. Views of the Density Field at t = 2.65 μs for K = 1

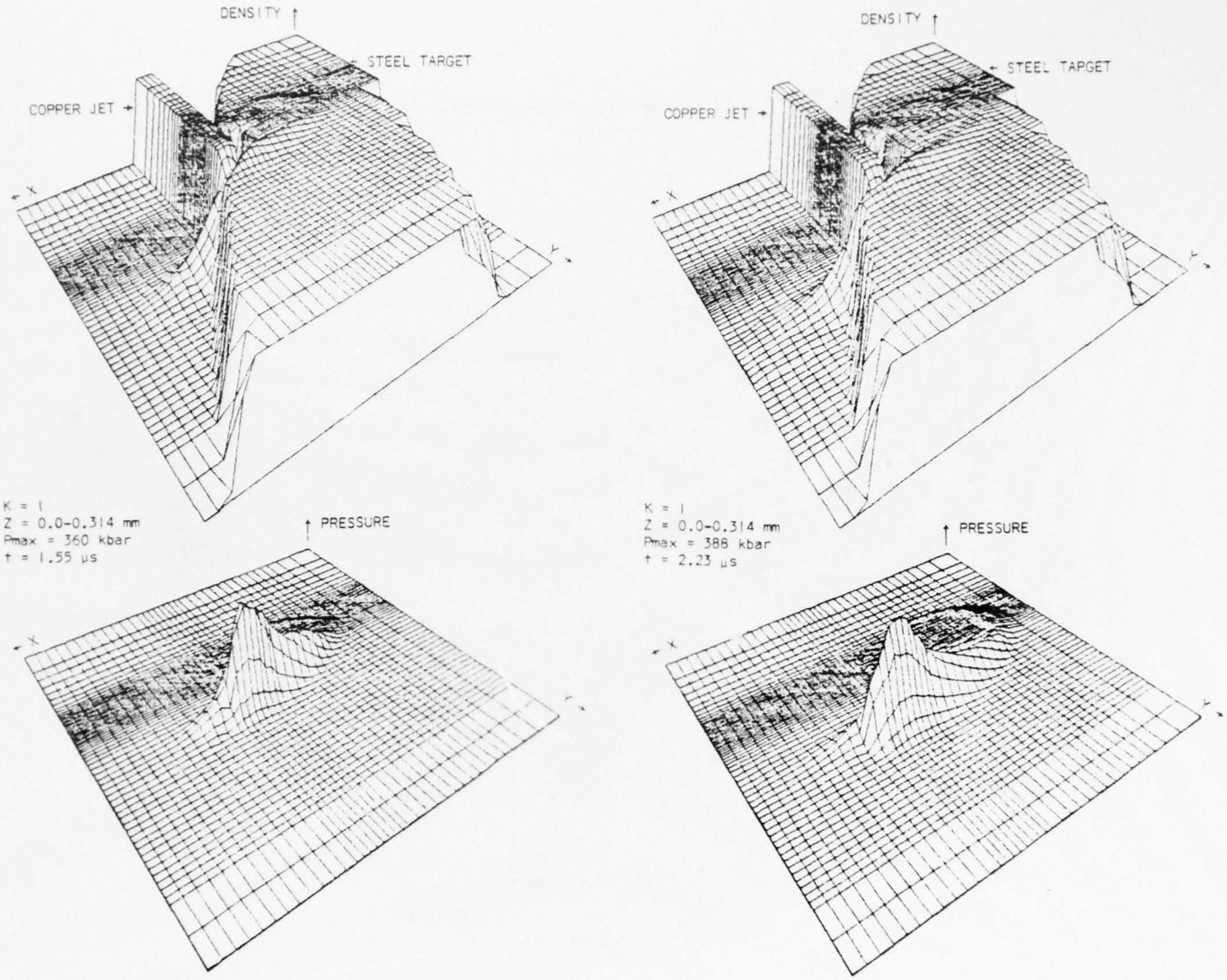

Figure 60. Density Field and Pressure Field Histories

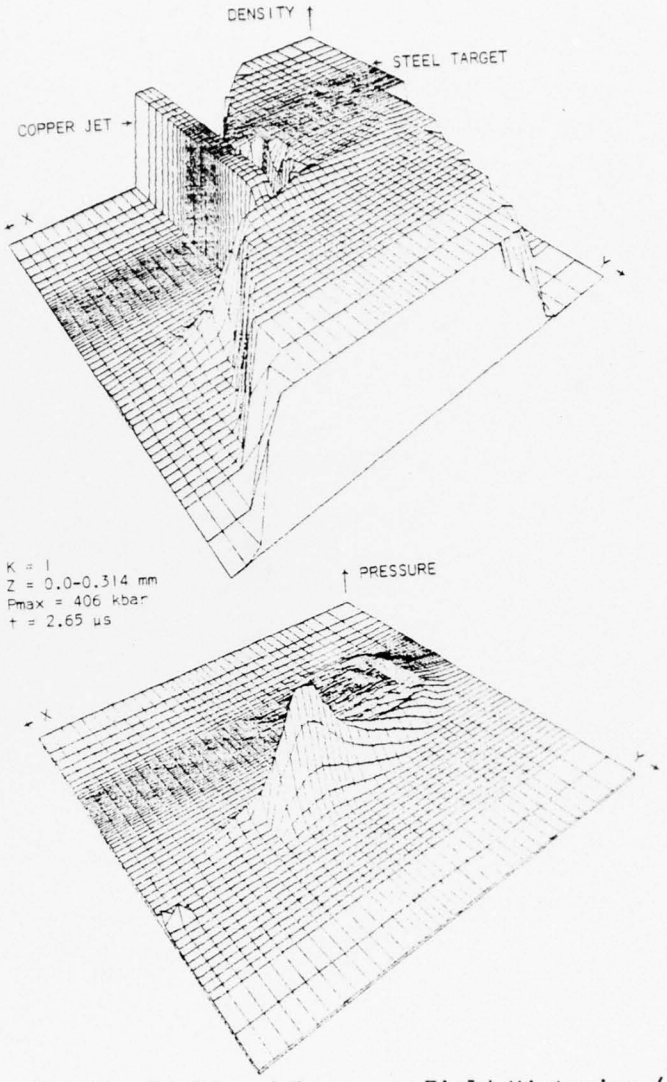

Figure 61. Density Field and Pressure Field Histories (continued)

DISTRIBUTION LIST

No. of Copies	Organization
12	Commander Defense Documentation Center ATTN: DDC-TCA Cameron Station Alexandria, VA 22314
1	Commander US Army Materiel Development and Readiness Command ATTN: DRCDMA-ST 5001 Eisenhower Avenue Alexandria, VA 22333
1	Commander US Army Aviation Research and Development Command ATTN: DRSAV-E 12th and Spruce Streets St. Louis, MO 63166
1	Director US Army Air Mobility Research and Development Laboratory Ames Research Center Moffett Field, CA 94035
1	Commander US Army Electronics Command ATTN: DRSEL-RD Fort Monmouth, NJ 07703
1	Commander US Army Tank Automotive Rsch & Development Command ATTN: DRDTA-RWL Warren, MI 48090
2	Commander US Army Mobility Equipment Research & Development Cmd ATTN: Tech Docu Cen, Bldg 315 DRSME-RZT Fort Belvoir, VA 22060
1	Commander US Army Missile Research and Development Command ATTN: DRDMI-R Redstone Arsenal, AL 35809
1	Commander US Army Armament Materiel Readiness Command ATTN: DRSAR-LEP-L, Tech Lib Rock Island, IL 61201
1	Commander US Army Harry Diamond Labs ATTN: DRXDO-TI 2800 Powder Mill Road Adelphi, MD 20783
1	Director US Army TRADOC Systems Analysis Activity ATTN: ATAA-SL, Tech Lib White Sands Missile Range NM 88002
	Aberdeen Proving Ground
	Marine Corps Ln Ofc Dir, USAMSAA